NOAA Technical Memorandum NMFS-AFSC-456

Evaluating Approaches to Estimating Mean Temperatures and Cold Pool Area from Alaska Fisheries Science Center Bottom Trawl Surveys of the Eastern Bering Sea

S. K. Rohan, L. A. K. Barnett, and N. Charriere

December 2022

U.S. DEPARTMENT OF COMMERCE

National Oceanic and Atmospheric Administration
National Marine Fisheries Service
Alaska Fisheries Science Center

The National Marine Fisheries Service's Alaska Fisheries Science Center uses the NOAA Technical Memorandum series to issue informal scientific and technical publications when complete formal review and editorial processing are not appropriate or feasible. Documents within this series reflect sound professional work and may be referenced in the formal scientific and technical literature.

The NMFS-AFSC Technical Memorandum series of the Alaska Fisheries Science Center continues the NMFS-F/NWC series established in 1970 by the Northwest Fisheries Center. The NMFS-NWFSC series is currently used by the Northwest Fisheries Science Center.

This document should be cited as follows:

Rohan, S. K., L. A. K. Barnett, and N. Charriere. 2022. Evaluating approaches to estimating mean temperatures and cold pool area from Alaska Fisheries Science Center bottom trawl surveys of the eastern Bering Sea. U.S. Dep. Commer., NOAA Tech. Memo. NMFS-AFSC-456, 42 p.

This document is available online at:

Document available: https://repository.library.noaa.gov

NOAA FISHERIES

Evaluating Approaches to Estimating Mean Temperatures and Cold Pool Area from Alaska Fisheries Science Center Bottom Trawl Surveys of the Eastern Bering Sea

S. K. Rohan, L. A. K. Barnett, and N. Charriere

Resource Assessment and Conservation Engineering Division
Alaska Fisheries Science Center
7600 Sand Point Way NE
Seattle, WA 98115

U.S. DEPARTMENT OF COMMERCE

National Oceanic and Atmospheric Administration
National Marine Fisheries Service
Alaska Fisheries Science Center

NOAA Technical Memorandum NOAA-TM-AFSC-456

December 2022

ABSTRACT

Water temperature data from the Alaska Fisheries Science Center's summer bottom trawl surveys of the eastern Bering Sea continental shelf and northern Bering Sea regions are used to generate regional temperature data products. These temperature data products are used in fishery stock assessment and management because temperature affects the distribution and productivity of regional fishes and invertebrates. However, methods for calculating these temperature data products (mean bottom temperature, mean surface temperature, cold pool extent) have not been detailed in the literature or compared with alternative methods. To address these shortcomings, we describe historical methods for calculating bottom trawl survey temperature data products using weighted means and inverse distance weighting interpolation and compare their predictive performance to alternative interpolation methods. Overall, we found strong agreement in regional temperature trends between historical and new methods, and only minor differences among methods for estimating mean bottom temperature (within 0.10 °C of historical), mean sea surface temperature (within 0.08 °C of historical), and cold pool extent. However, we recommend using ordinary kriging interpolation because this method ranked highest by our performance metrics. These estimates are provided as built-in datasets in the R package *coldpool* (https://github.com/afsc-gap-products/coldpool).

CONTENTS

INTRODUCTION

The eastern Bering Sea is a highly productive ecosystem that supports large populations of marine mammals, seabirds, fishes, and invertebrates, as well as the subsistence, commercial, and recreational harvest of these animals. The distribution and productivity of these populations is greatly influenced by water temperature (Kotwicki and Lauth 2013, Spencer et al. 2016, Duffy-Anderson et al. 2019) and, as such, water temperature data are used as covariates in stock assessment models and provide contextual information to the North Pacific Fishery Management Council (NPFMC) in support of ecosystem-based fisheries management. An important source of temperature data for stock assessment and management is the Alaska Fisheries Science Center's annual summer (May–August) bottom trawl survey of the eastern Bering Sea continental shelf that has collected temperature, a suite of other environmental data, and biological (species abundance, demography, diet) data using a standardized survey design since 1982. The survey's simultaneous observations of environmental and biological data facilitates inference into effects of temperature on populations and communities of demersal macrofauna.

In the eastern Bering Sea, seasonal sea ice that forms during winter and melts in spring has a strong influence on sea temperature patterns during the subsequent summer and fall (Stabeno et al. 2012). Years with extensive sea ice cover that persists until late spring are associated with colder temperatures across most of the shelf region, while years with limited sea ice cover and early retreat are associated with warmer temperatures. Temperature strongly influences thermal stratification (Ladd and Stabeno 2012), and overall, changes in surface and bottom temperature influence the spatial structure of pelagic and demersal communities (Spencer 2008, Kotwicki and Lauth 2013, Stabeno et al. 2012, Thorson et al. 2020), trophic structure of the eastern Bering Sea food web (Mueter and Litzow 2008, Spencer et al. 2016), and demographic processes of fish populations (Grüss et al. 2021). The cold water mass that forms near the seafloor as a result of sea ice melting is commonly referred to as the "cold pool." When this cold pool is small, species with warm-water affinity (e.g., arrowtooth flounder (*Atheresthes stomias*)) are distributed more widely over the eastern Bering Sea shelf and expand across the shelf and to the north. In contrast, the distribution of species with cold water affinity (e.g., Arctic cod (*Boreogadus saida*), Bering flounder (*Hippoglossoides robustus*)) contracts to the north when the cold pool is small (Kotwicki and Lauth 2013, Baker 2021). These concomitant changes in species distribution and temperature, in combination with changes in productivity and mortality greatly influence demersal community structure in Pacific Arctic and subarctic waters.

The cold pool extent (i.e., cold pool area) index was initially developed as a summary metric describing the two-dimensional thermal structure of the demersal ecosystem of the southeastern Bering Sea continental shelf from Alaska Fisheries Science Center's (AFSC) annual summer bottom trawl survey temperature measurements. The index is defined as the total area of the southeastern Bering Sea continental shelf bottom trawl survey area where bottom temperatures are less than or equal to 2°C, in units of square kilometers (km^2). The summer cold pool extent has historically shown considerable interannual variability. The mean cold pool

area from 1982 to 2019 was 186,626 km^2, with a maximum area of 393,595 km^2 in 1999, and minimum area of 6,924 km^2 in 2019 (Siddon 2021).

Mean bottom temperature and cold pool extent data products from bottom trawl surveys have been widely used in ecological research and stock assessment. Variability in bottom trawl survey mean bottom temperature and cold pool extent have been linked to variation in demographic rates (recruitment and mortality), proxies for the outcome of demographic rates (e.g., weight-at-age, weight-at-length), and spatial patterns of species distribution and predator-prey interactions (Cooper et al. 2020, Mueter et al. 2006, Grüss et al. 2021, Siddon et al. 2013, Spencer et al. 2016, Thorson et al. 2020). Mean survey bottom temperature (Ianelli et al. 2001) and mean bottom temperature at survey stations < 100 m (Wilderbuer and Nichol 2001) have been used as inputs in fisheries stock assessment models to estimate catchability of bottom trawl surveys since the early 2000s because bottom temperature and cold pool extent are thought to influence the spatial distribution and migration timing of fish stocks (Bakkala 1981, Francis and Bailey 1983, Wyllie-Echeverria and Wooster 1998). Cold pool extent and mean bottom temperature have also been used for ecological process research that seeks to improve qualitative and quantitative understanding of how variation in the thermal structure of the water column influences faunal distributions and demographic rates, and ultimately how the community structure and function is delineated across this physiological biogeographic boundary (Spencer 2008, Kotwicki and Lauth 2013, Stabeno et al. 2012, Eisner et al. 2020, Nichol et al. 2019, Thorson et al. 2020). The myriad uses of bottom trawl survey cold pool extent and temperature products underscores the importance of ensuring these products are calculated using accurate, consistent, and reproducible methods in accordance with the best available science.

Although mean temperature and cold pool extent data products from the eastern Bering Sea shelf bottom trawl survey have been used as indicators of ecosystem conditions since the late 1990s (Livingston 1999, Boldt and Zador 2009), the specific methods used to calculate these metrics have been poorly documented. Herein, we describe the historical methods of collecting temperature data and estimating average bottom temperature, surface temperature, and cold pool area from these data. We then compare temperature estimates and predictive performance of the historical methods to those calculated using a suite of candidate interpolation methods that have the potential to produce more accurate and precise estimates of bottom temperature, sea surface temperature, and cold pool extent. Based on the results of the comparison, we recommend a new, open source method for calculating and distributing cold pool area and mean bottom and surface temperature data products in an R package, *coldpool* (https://github.com/afsc-gap-products/coldpool). The package includes built-in temperature data products and visualizations that are useful for fisheries stock assessments and management in the eastern Bering Sea. The data products are derived from observations from standard survey stations of the AFSC eastern Bering Sea shelf bottom trawl survey (conducted from late May to late July), and in some cases include observations from the AFSC northern Bering Sea shelf bottom trawl survey (conducted during August).

MATERIALS AND METHODS

Bottom Trawl Surveys in the Eastern Bering Sea

Temperature data from the eastern Bering Sea continental shelf are collected during the Alaska Fisheries Science Center's standardized bottom-trawl surveys of the eastern Bering Sea continental shelf (EBS shelf) and northern Bering Sea (NBS) survey areas. Detailed descriptions of trawl survey protocols can be found in Stauffer (2003) and Lauth et al. (2019; EBS shelf and NBS). A brief summary of survey sampling procedures is described below.

The Alaska Fisheries Science Center has conducted summer (late May–early August) bottom-trawl surveys of the eastern Bering Sea continental shelf annually since 1982[1]. Observations collected during this survey provide the data used to generate survey temperature products. Every year, sampling has been conducted at 376 index stations arranged on a regularly spaced systematic sampling grid with 37.04 × 37.04 km (20 nmi × 20 nmi) grid cells (Fig. 1). The survey design grid has changed over time: stations were added to the northwest (strata 82 and 90) portion of the survey grid in 1985 and corner stations were added in 1987 around St. Paul Island, St. George Island, and St. Matthew Island in areas that historically had high densities of red king crab (*Paralithodes camtschaticus*) and blue king crab (*Paralithodes platypus*) (Fig. 1). Two chartered commercial trawl vessels are used to conduct each survey. Survey sampling begins in the interior waters of Bristol Bay and moves northwest over an average of 57 days.

The NBS survey is conducted from late July to mid-August and samples 144 index stations arranged on a regularly spaced systematic sampling grid with 37.04 × 37.04 km (20 nmi × 20 nmi) grid cells (Fig. 1). The NBS survey is an extension of the EBS shelf survey and begins at stations adjacent to where the EBS shelf finishes sampling in strata 82 and 90. The NBS survey progresses northward and inshore towards the Bering Strait and Norton Sound before heading south and finishing around Nunivak Island, which takes an average of 26 days. A portion of the NBS survey area was also sampled in 2018 for a rapid response survey that was conducted due to changes in the spatial distribution of Pacific cod (*Gadus macrocephalus*) that were associated with unusually warm bottom temperatures and a small cold pool. The NBS survey was conducted by three vessels in 2010 and two vessels in 2017, 2019, and 2021.

[1] Except 2020 due to the COVID-19 pandemic.

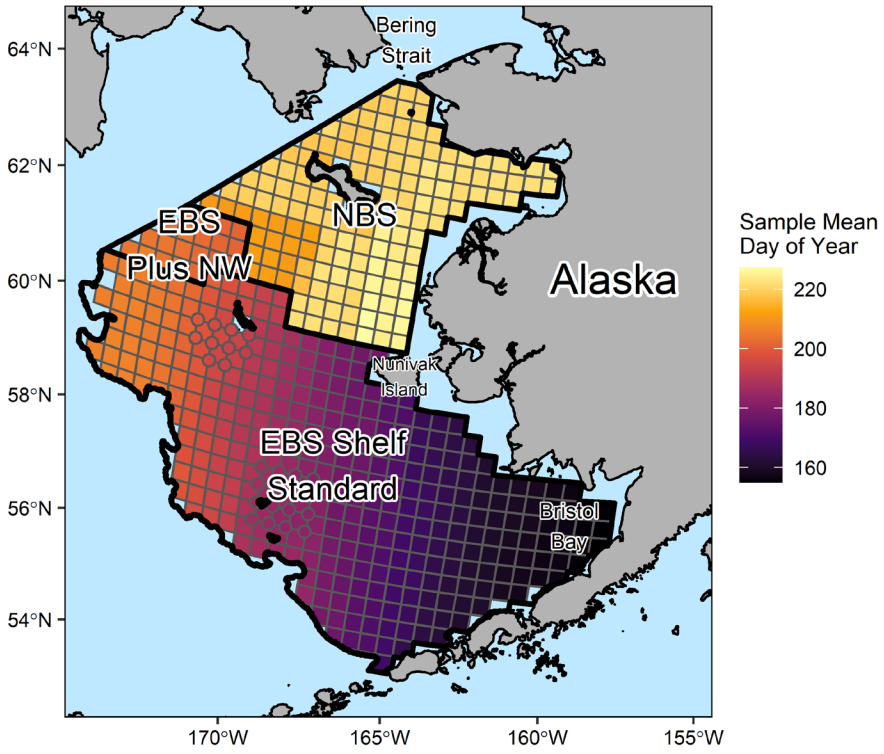

Figure 1. -- Map of the Alaska Fisheries Science Center, Resource Assessment and Conservation Engineering Division's eastern Bering Sea shelf (EBS Standard and EBS NW) and northern Bering Sea (NBS) survey areas and station grids. Fill color denotes the mean day of year a station is sampled.

Temperature Data Collection and Processing

Methods for collecting water temperature data have changed over time (Table 1). From 1982 to 1992, water column temperature measurements were mainly collected by deploying an expendable bathythermograph (XBT) at each survey station. The XBT used graph paper traces on both vessels from 1982 to 1989, graph paper traces on one vessel and digital traces on the other vessel in 1990, and digital traces on both vessels from 1991 to 1992.

From 1993 to present, water column temperature data have been collected using a digital temperature-depth recorder (TDR; i.e., micro-bathythermograph) attached to the outside of the top panel of the trawl gear. At the beginning of each haul, the TDR remains just below the sea surface for 2–5 minutes while the gear is set up for trawling. Presumably, holding the TDR at the surface allows temperature measurements to equilibrate towards sea surface temperature. TDR bottom temperature data from the EBS shelf and NBS are collected from

~2.3 m above the seafloor, the average height of an 83-112 bottom trawl in fishing configuration (von Szalay and Somerton 2005).

Sea surface temperature (SST) sampling methods have changed over time and sampling equipment used to measure surface and bottom temperatures differed prior to 2006. From 1982 to 1991 and 1993 to 2005, SST data were primarily obtained from surface bucket samples using a mercury thermometer (Table 1). In 1992, SST data were collected using a thermometer lowered to the sea surface. From 2006 to 2013, SST was estimated from TDR data by using graphical software to manually select the temperature measurement from the closest depth to 1 m, immediately prior to the beginning of the downcast. Since 2013, a software algorithm has been used to estimate SST at 1 m from TDR data. Using the algorithm, SST is taken to be the first measurement during the upcast where depth is equal to 1 m (rounded to the nearest 0.2 m). If a depth less than 1 m is recorded before a 1 m depth, temperature at 1 m is estimated by linearly interpolating between the temperature measurement from the first upcast depth shallower than 1 m and last depth deeper than 1 m.

The number of temperature samples collected varied among years for both the EBS and NBS surveys (Table 2) due to factors such as changes in the number of stations and equipment malfunction. When temperature measurements from the primary sensor are missing from the bottom or surface, measurements from backup temperature sensors are used when available. Examples of backup sensors have been trawl-mounted CTD units (e.g., Teledyne Citadel CTD-NV, NXIC CTD, Aanderaa SeaGuard CTD recorder, SBE19plus CTD), temperature-logging trawl spread sensors (e.g., Marport High-Definition Trawl Explorer), and XBTs.

Historical Mean Bottom and Surface Temperature Calculations

Historically, EBS shelf mean bottom and surface temperatures were calculated using a weighting method based on the areas of EBS shelf survey strata. For this method, bottom or surface temperatures from standard EBS shelf index stations were averaged and proportionally weighted based on the area of the stratum in which they were collected. The equation for calculating mean temperature using this method was

$$T_d = \sum_{s=1}^{n_s} \sum_{i=1}^{n_i} \frac{A_s T_{d,s,i}}{A n_i},$$

where T_d is temperature at depth layer *d* (bottom or surface), A_s is the area of survey stratum *s*, *A* is the total area of the EBS shelf survey area, n_s is the number of survey strata, and n_i is the number of temperature samples (i.e., successful index station standard hauls) within a stratum.

The number of temperature samples from each EBS shelf survey stratum varied among years due to changes in the number of stations and factors such as equipment malfunction, as described in the previous section, which can lead to undesirable artifacts in temperature data products. In some years (e.g., 1990), stations with missing temperature data were spatially clustered, thereby increasing the relative influence of stations from other portions of the stratum on mean temperature calculations. A more robust way of estimating temperatures at unobserved locations than the area weighting method would be to use spatial interpolation methods that account for the spatial structure among samples, both within and across stratum boundaries.

Table 1. -- Equipment and methods used to collect water temperature data in the eastern Bering Sea and northern Bering Sea, by year and depth layer.

Years	Layer	Equipment	Calculation Method
1982–1990[a]	Water column and bottom	Expendable bathythermograph (XBT) with graph paper traces	Graphical selection from deepest temperature measurement
1983–1984[b,c] (one vessel)	Water column and bottom	CTD cast	Graphical selection from deepest temperature measurement
1990–1992[d,e]	Water column and bottom	XBT with digital traces	Graphical selection from deepest temperature measurement
1992–2021[d,e,g]	Water column and bottom	trawl-mounted temperature depth recorder (TDR)	Average temperature between trawl on-bottom and haul back times
1982–2005[d,e,f]	Surface	Bucket sample with thermometer	Bucket thermometer temperature
1983–1984[b,c] (one vessel)	Surface	CTD cast	Graphical selection from cast profile
1992[d,e]	Surface	Thermometer lowered to sea surface	Surface thermometer temperature
2006–2013[g]	Surface	trawl-mounted TDR	Graphically-assisted selection of 1-m downcast temperature
2013–2021	Surface	trawl-mounted TDR	Algorithmically calculated 1-m upcast temperature

[a]-Bakkala et al. (1985), [b]-U.S. Department of Commerce (1983); [c]-U.S. Department of Commerce (1984); [d]-U.S. Department of Commerce (1992); [e]-Walters (1996); [f]-Lauth and Acuna (2007a); [g]-Lauth and Acuna (2007b)

Table 2. -- Summer bottom-trawl survey survey sampling dates and number of stations with bottom (N_B) and surface (N_S) temperature data in the eastern Bering Sea and northern Bering Sea from 1982 to 2021.

	Eastern Bering Sea Shelf			Northern Bering Sea		
Year	**Dates**	**N_B**	**N_S**	**Dates**	**N_B**	**N_S**
1982	May 29–Aug 1	328	328	-	-	
1983	Jun 7–Aug 1	351	350	-	-	
1984	Jun 10–Aug 19	346	346	-	-	
1985	Jun 8–Sep 10	312	309	-	-	
1986	Jun 3–Aug 1	343	341	-	-	
1987	May 27–Jul 30	353	265	-	-	
1988	Jun 4–Jul 30	371	366	-	-	
1989	Jun 6–Aug 11	361	351	-	-	
1990	Jun 5–Aug 1	307	303	-	-	
1991	Jun 7–Aug 13	335	312	-	-	
1992	Jun 6–Aug 3	314	301	-	-	
1993	Jun 4–Jul 26	333	330	-	-	
1994	Jun 3–Jul 26	291	291	-	-	
1995	Jun 4–Jul 22	353	353	-	-	
1996	Jun 8–Jul 28	363	363	-	-	
1997	Jun 7–Jul 26	355	355	-	-	
1998	Jun 9–Jul 29	351	349	-	-	
1999	May 23–Jul 11	348	348	-	-	
2000	May 23–Jul 20	348	343	-	-	
2001	May 29–Jul 19	361	357	-	-	
2002	Jun 2–Jul 24	366	363	-	-	
2003	Jun 2–Jul 22	368	368	-	-	
2004	Jun 5–Jul 25	367	366	-	-	

	Eastern Bering Sea Shelf			Northern Bering Sea		
Year	**Dates**	**N_B**	**N_S**	**Dates**	**N_B**	**N_S**
2005	Jun 3–Jul 22	347	347	-	-	
2006	Jun 2–Jul 25	370	370	-	-	
2007	Jun 11–Jul 28	376	375	-	-	
2008	Jun 4–Jul 24	375	375	-	-	
2009	Jun 2–Jul 19	376	376	-	-	
2010	Jun 7–Aug 4	376	376	Jul 23–Aug 10	141	141
2011	Jun 5–Jul 25	376	376	-	-	
2012	Jun 4–Jul 25	374	374	-	-	
2013	Jun 9–Aug 1	376	376	-	-	
2014	Jun 8–Aug 2	376	376	-	-	
2015	Jun 2–Jul 29	376	376	-	-	
2016	May 31–Jul 26	376	376	-	-	
2017	Jun 4–Jul 31	376	376	Aug 1–Sep 2	143	143
2018	Jun 3–Jul 31	375	375	-	-	
2019	Jun 3–Jul 28	376	375	Jul 28–Aug 20	144	144
2020	-	-	-	-	-	-
2021	May 31–Jul 22	376	375	Jul 22–Aug 16	144	144

Historical Cold Pool Area Calculations

EBS shelf cold pool area was historically calculated from spatially interpolated bottom temperatures that were derived from standard EBS shelf index stations. Spatial interpolation and area calculations were performed using proprietary software (Esri ArcGIS) and analysts manually configured software settings to calculate cold pool area each year. To calculate cold pool area, georeferenced temperature data from surveys were projected to the North American Datum 1983 Alaska Albers Equal Area (NAD83) projection (i.e., European Petroleum Survey Group [EPSG] projection 3338). Temperature was interpolated on a grid using inverse distance weighting with power equal to 2.0. The grid for interpolation was set to have 250 cells

along the longest axis of the interpolation region. At each prediction location, only the four closest samples were used to estimate temperature. Grids were then masked to the survey extent and total areas were calculated for polygons defining the bottom temperature ≤ -1°C, ≤ 0°C, ≤ 1°C, and ≤ 2°C (cold pool) isotherms. While data used for spatial interpolation were chosen to minimize effects of non-stationarity in survey sampling, the spatial interpolation method was used because it is the default setting for spatial interpolation in ArcGIS. As such, it is worth considering that other spatial interpolation methods may have higher out-of-sample prediction skill (i.e., prediction at unsampled grid cells) that may improve the accuracy of estimates of areas with bottom temperatures ≤ -1°C, ≤ 0°C, ≤ 1°C, and ≤ 2°C.

Historical estimates of cold pool area are difficult to reproduce, presumably because methods for calculating EBS shelf cold pool area sometimes deviated from the procedure described above. This likely occurred due to factors such as configuring software settings differently among years or including data from non-standard samples (e.g., crab resample stations in Bristol Bay). A reproducible method for calculating cold pool area would improve the quality and consistency of the cold pool area data product.

Proposed Methods for Calculating Mean Surface Temperature, Mean Bottom Temperature, and Cold Pool Area

We sought to develop consistent, reproducible, and robust methods for calculating survey temperature products (mean bottom temperature, mean surface temperature, and cold pool area). To do so, we evaluated the out-of-sample predictive performance of spatial interpolation methods at predicting bottom and surface temperatures using interpolation methods from open source software. We used the best performing candidate spatial interpolation to generate bottom and surface temperature grids for the EBS shelf and used the grids to calculate mean bottom temperature for the EBS shelf, mean surface temperature for the EBS shelf, and EBS shelf area with bottom temperatures ≤ -1°C, ≤ 0°C, ≤ 1°C, and ≤ 2°C. Below, we describe the spatial interpolation methods that we compared, our approach to evaluating out-of-sample predictive performance of interpolation methods using cross-validation, and the data used for interpolation.

The candidate interpolation methods we considered were nearest neighbor interpolation, inverse distance weighting interpolation (power = 2) without proximity constraints (IDW), ordinary kriging interpolation with seven different candidate semivariogram models (exponential, Gaussian, circular, spherical, Bessel, Matérn, and Stein's Matérn), and thin-plate splines. We did not model anisotropy in nearest neighbor, IDW, or ordinary kriging methods. Nearest neighbor, IDW, and ordinary kriging were conducted using the R package *gstat* (Pebesma 2004).

We compared the performance of candidate interpolation methods using leave-one-out cross validation to quantify the out-of-sample predictive error of each method for each survey year.

We considered the best method for a year to be the method with the lowest root-mean-square prediction error (RMSPE),

$$RMSPE_y = N_y^{-1} \sum_{i=1}^{N_y} \sqrt{\left(\widehat{T}_i - T_i\right)^2},$$

where y is year, N_y is the number of temperature samples in year y, i is the sample index, and $\widehat{T}_i$ and T_i are the predicted and observed temperatures (°C) for sample i. We considered the best method among years to be the interpolation method that had the highest number of years with the best performance (lowest RMSPE).

Temperature data used for interpolation were collected from standard index station samples collected during the EBS shelf survey to ensure data were comparable to those collected in other years. Northern Bering Sea sample stations were omitted due to a positive (i.e., warm) bias along the boundary between the EBS shelf and NBS survey areas. This bias occurs because the southern NBS stations around Nunivak Island are sampled at the end of the survey and undergo solar heating during the summer. Temperature data from non-standard hauls (e.g. red king crab resample stations, gear experiments) were omitted to mitigate potential sampling biases caused by sampling at the end of surveys.

RESULTS

The best spatial interpolation method for bottom temperature was ordinary kriging with a Stein's Matérn variogram, based on root mean square prediction errors (RMSPEs) from leave-one-out cross-validation. This method had the best predictive performance among candidate interpolation methods in 13 out of 34 years; ordinary kriging with a Matérn variogram was second best with the best performance in 8 out of 34 years (Table 3). However, ordinary kriging with Stein's Matérn, Matérn, and exponential variograms were nearly tied for the best (lowest) out-of-sample predictive performance across all years, as their mean RMSPEs were rounded to 0.324 °C. Inverse distance weighting, the method previously used to interpolate bottom temperatures for cold pool area calculations, had the second worst predictive performance and had a mean RMSPE approximately double (0.646 °C) the RMSPE of the best-performing candidate interpolation methods (Table 3). The year with the worst (highest) RMSPE was 1984 for most methods, while the year with the best (lowest) RMSPE was 2018 for most methods (Table 3).

Estimates of mean bottom temperature from all interpolation methods were within 0.12°C of each other within each year (Fig. 2A), which indicates all methods yield similar trends and scale. These estimates were also within 0.1°C of mean bottom temperature estimates from area-weighted interpolation, aside from a few cases between 1992 and 1994 (Fig. 2B). Rankings of mean bottom temperatures by year were nearly identical among methods as all between-method rank-order correlations > 0.99 (Kendall's τ; Table 4).

Based on the number of years with the lowest RMSPE, the best spatial interpolation method for sea surface temperature was inverse distance weighting using only the four nearest observations (IDW-NMAX4; 16 out of 34 years) followed by thin-plate spline (9 out of 34 years; Table 5). IDW-NMAX4 had the best (lowest) mean RMSPE among years (0.436 °C), although similar performance was achieved by ordinary kriging with Stein's Matérn (0.440 °C), Matérn (0.440 °C), exponential (0.440 °C), and spherical (0.441 °C) variograms (Table 5). All interpolation methods yielded estimates of mean sea surface temperature within 0.1°C of each other (Fig. 3A) and within 0.08°C of the estimate from the area-weighting method (Fig. 3B), which indicates all methods yield highly similar trends and scale. The year with the worst (highest) RMSPE was 1982 for most methods and the year with the best (lowest) RMSPE was 2018 for most methods (Table 5). Rankings of annual mean sea surface temperatures were extremely similar among methods $\tau > 0.97$ (Table 6).

Estimates of cold pool area were similar among methods as shown by similar trends and scale among methods (Fig. 4A) and high correlation ($\tau > 0.91$) of cold pool area rankings between methods (Table 7). Among methods, cold pool area estimates based on inverse distance weighting without nearest neighbor constraints had the largest differences from other candidate interpolation methods and historical estimates of cold pool area (Fig. 4A, B). Inverse distance weighting interpolation with only the four closest samples used for interpolation (IDW-NMAX4), the method historically used to calculate cold pool area in ArcMap, had the closest agreement with the historical cold pool area data product and annual rankings of cold pool area (highest Kendall's τ; Table 7).

Interpolation Method for Data Products

Based on results of our comparisons, we selected ordinary kriging with a Stein's Matérn variogram as the spatial interpolation method to use to produce bottom temperature, sea surface temperature, and cold pool area data products. Ordinary kriging with a Stein's Matérn variogram was the best performing interpolation method for bottom temperature because it had the most years with the lowest RMSPE and the lowest mean RMSPE among methods. Because cold pool area is calculated from bottom temperature, ordinary kriging with Stein's Matérn also had the best performance among methods for estimating cold pool area. Although ordinary kriging with a Stein's Matérn variogram ranked below IDW-NMAX4 and thin-plate spline for the number of years with the lowest RMSPE for sea surface temperature, its RMSPE was within 0.005 of IDW-NMAX4 and above that of thin plate spline. Ordinary kriging with a Stein's Matérn variogram and IDW-NMAX4 had similar estimates of mean sea surface temperature and identical rankings of annual mean sea surface temperature ($\tau = 1.0$; Table 6). Considering close agreement between methods, we selected ordinary kriging with a Stein's Matérn variogram to calculate sea surface temperature data products because it is a geostatistical method (as opposed to inverse distance weighting, which is a deterministic exact interpolator) and to match the method used for bottom temperature and cold pool area.

Notably, exact interpolators, such as inverse distance weighting, have discontinuities at prediction locations, tend to produce sharp peaks and troughs, and are sensitive to outliers.

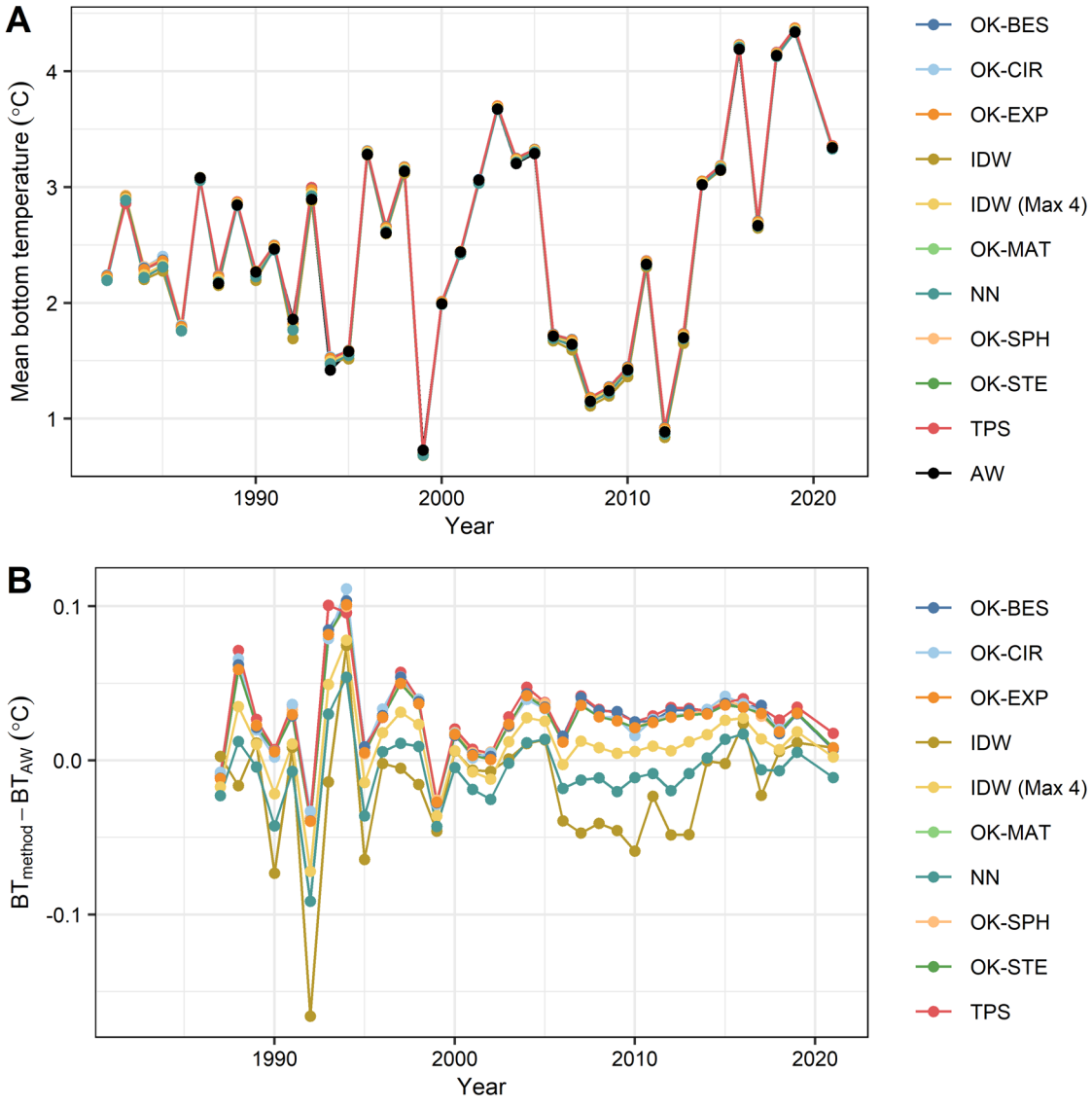

Figure 2. -- Mean bottom temperature (BT; °C) in the eastern Bering Sea shelf bottom trawl survey area for different estimation methods from 1987 to 2021. Panels show: (A) estimates from candidate spatial interpolation methods and area-weighted method, (B) difference between BT from candidate methods and value from area weighting. Line and point colors denote the interpolation method: OK = ordinary kriging, BES = Bessel, CIR = circular, EXP = exponential, MAT = Matérn, SPH = spherical, STE = Stein's Matérn, IDW = inverse distance weighting, IDW (Max 4) = inverse distance weighting with only four closest observations used for prediction, NN = nearest neighbor, TPS = thin plate spline, AW = area-weighting.

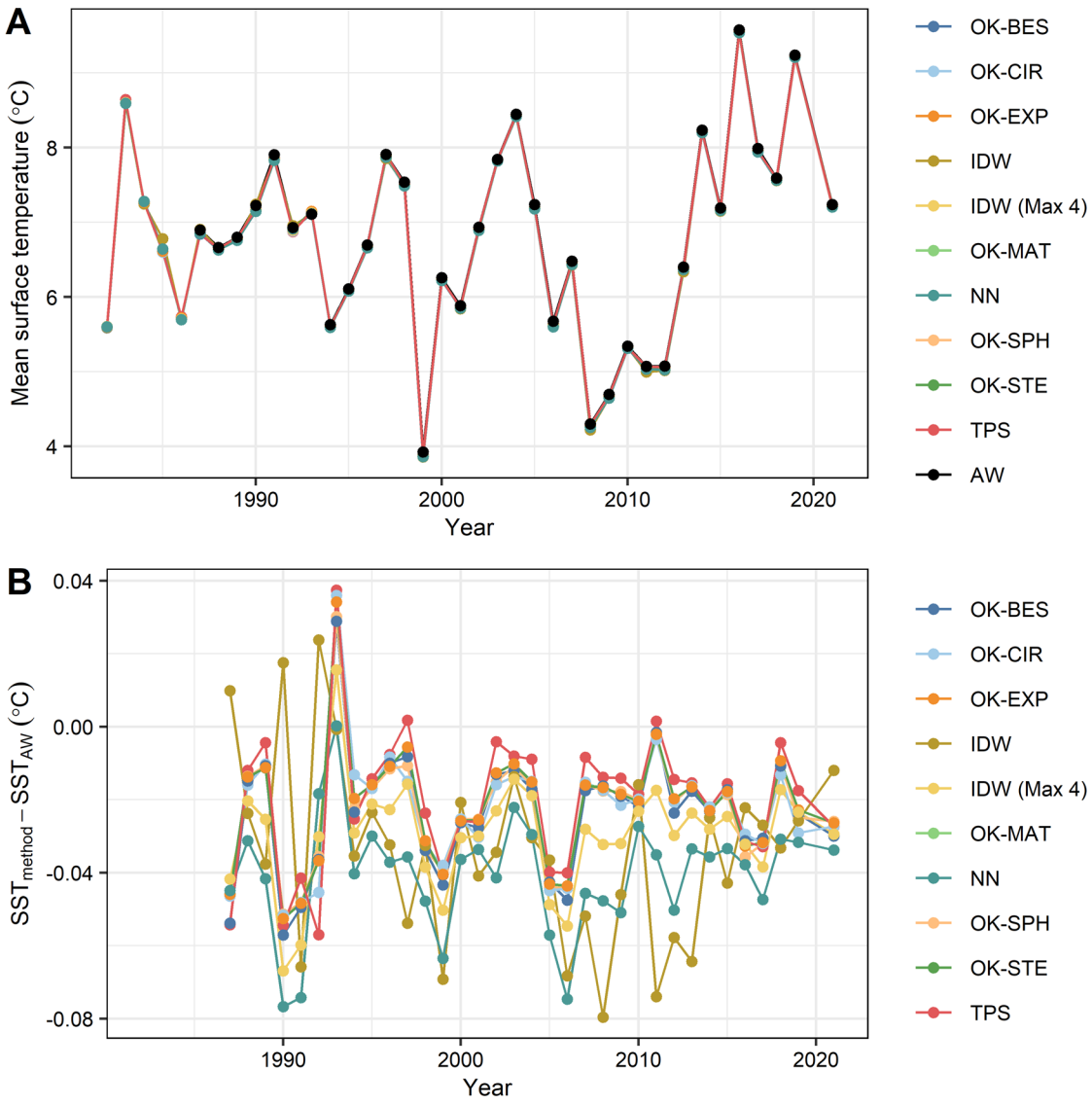

Figure 3. -- Mean sea surface temperature (SST; °C) in the eastern Bering Sea shelf bottom trawl survey area for different estimation methods from 1987 to 2021. Panels show: (A) estimates from candidate spatial interpolation methods and area-weighted method, (B) difference between SST from candidate methods and value from area weighting. Line and point colors denote the interpolation method: OK = ordinary kriging, BES = Bessel, CIR = circular, EXP = exponential, MAT = Matérn, SPH = spherical, STE = Stein's Matérn, IDW = inverse distance weighting, IDW (Max 4) = inverse distance weighting with only four closest observations used for prediction, NN = nearest neighbor, TPS = thin plate spline, AW = area-weighting.

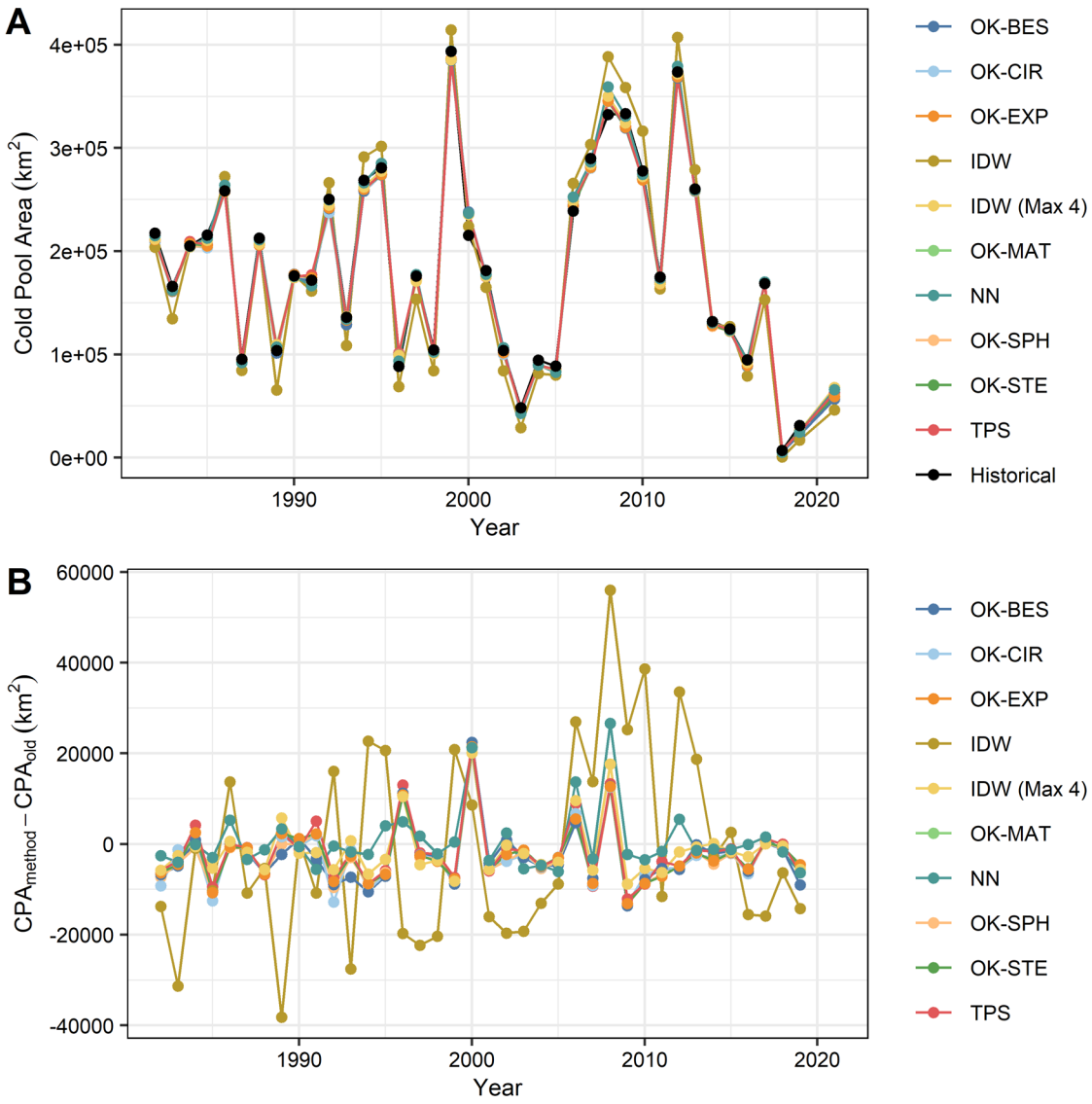

Figure 4. -- Cold pool area (CPA; km^2) in the eastern Bering Sea shelf bottom trawl survey area for different estimation methods from 1982 to 2021. Panels show: (A) estimates from candidate spatial interpolation methods and the historical value obtained from GIS software, (B) difference between CPA from candidate methods and historical (old) value. Line and point colors denote the interpolation method: OK = ordinary kriging, BES = Bessel, CIR = circular, EXP = exponential, MAT = Matérn, SPH = spherical, STE = Stein's Matérn, IDW = inverse distance weighting, IDW (Max 4) = inverse distance weighting with only four closest observations used for prediction, NN = nearest neighbor, TPS = thin plate spline.

Table 3. -- Bottom temperature root-mean-square prediction error (RMPSE) from leave-one-out cross-validation.

	RMSPE (°C)						
Method	**Mean**	**SD**	**Min.**	**Max**	**Max. Yr.**	**Min. Yr.**	**No. Best**
NN	1.310	0.244	0.819	1.770	2015	2018	0
IDW	0.646	0.145	0.373	0.939	1984	2021	0
IDW (Max 4)	0.350	0.076	0.224	0.622	1984	2018	0
EXP	0.324	0.076	0.202	0.598	1984	2018	1
SPH	0.326	0.077	0.204	0.602	1984	2018	5
CIR	0.339	0.081	0.206	0.615	1984	2018	2
GAU	0.386	0.076	0.271	0.651	1984	2018	0
BES	0.331	0.075	0.214	0.600	1984	2018	5
MAT	0.324	0.076	0.202	0.598	1984	2018	8
STE	0.324	0.076	0.202	0.598	1984	2018	13
TPS	0.327	0.079	0.207	0.599	1984	2018	5

Table 4. -- Rank order correlation (Kendall's tau) of annual bottom temperature estimates among methods. AW = area-weighted mean, OK = ordinary kriging, BES = Bessel, CIR = circular, EXP = exponential, MAT = Matérn, SPH = spherical, STE = Stein's Matérn, IDW = inverse distance weighting, IDW (Max 4) = inverse distance weighting with only four closest observations used for prediction, NN = nearest neighbor, TPS = thin plate spline.

Method	AW	IDW	IDW (Max 4)	NN	OK-BES	OK-CIR	OK-EXP	OK-MAT	OK-SPH	OK-STE
IDW	0.996	-	-	-	-	-	-	-	-	-
IDW (Max 4)	0.993	0.996	-	-	-	-	-	-	-	-
NN	0.996	1	0.996	-	-	-	-	-	-	-
OK-BES	0.993	0.996	1	0.996	-	-	-	-	-	-
OK-CIR	0.993	0.996	1	0.996	1	-	-	-	-	-
OK-EXP	0.993	0.996	1	0.996	1	1	-	-	-	-
OK-MAT	0.993	0.996	1	0.996	1	1	1	-	-	-
OK-SPH	0.993	0.996	1	0.996	1	1	1	1	-	-
OK-STE	0.993	0.996	1	0.996	1	1	1	1	1	-
TPS	0.993	0.996	1	0.996	1	1	1	1	1	1

Table 5. -- Sea surface temperature root-mean square prediction error (RMPSE) from leave-one-out cross validation. OK = ordinary kriging, BES = Bessel, CIR = circular, EXP = exponential, MAT = Matérn, SPH = spherical, STE = Stein's Matérn, IDW = inverse distance weighting, IDW (Max 4) = inverse distance weighting with only four closest observations used for prediction, NN = nearest neighbor, TPS = thin plate spline.

	RMSPE (°C)						
Method	**Mean**	**SD**	**Min**	**Max**	**Max. Year**	**Min. Year**	**No. Best**
NN	1.412	0.295	0.858	1.955	2010	1983	0
IDW	0.640	0.093	0.462	0.855	2006	2018	0
IDW (Max 4)	0.436	0.074	0.294	0.595	1988	2018	16
OK-EXP	0.440	0.082	0.299	0.643	1982	2018	1
OK-SPH	0.441	0.083	0.307	0.642	1982	2018	3
OK-CIR	0.447	0.083	0.316	0.642	1982	2018	3
OK-GAU	0.529	0.092	0.385	0.724	1982	2011	0
OK-BES	0.456	0.085	0.321	0.664	1982	2018	1
OK-MAT	0.440	0.082	0.299	0.643	1982	2018	2
OK-STE	0.440	0.082	0.299	0.643	1982	2018	4
OK-TPS	0.444	0.086	0.279	0.663	1982	2018	9

Table 6. -- Rank order correlation (Kendall's tau) of annual sea surface temperature estimates among methods. AW = area-weighted mean, OK = ordinary kriging, BES = Bessel, CIR = circular, EXP = exponential, MAT = Matérn, SPH = spherical, STE = Stein's Matérn, IDW = inverse distance weighting, IDW (Max 4) = inverse distance weighting with only four closest observations used for prediction, NN = nearest neighbor, TPS = thin plate spline.

Method	AW	IDW	IDW (Max 4)	NN	OK-BES	OK-CIR	OK-EXP	OK-MAT	OK-SPH	OK-STE
IDW	0.986	-	-	-	-	-	-	-	-	-
IDW (Max 4)	0.993	0.979	-	-	-	-	-	-	-	-
NN	0.989	0.982	0.996	-	-	-	-	-	-	-
OK-BES	0.993	0.979	1	0.996	-	-	-	-	-	-
OK-CIR	0.993	0.979	1	0.996	1	-	-	-	-	-
OK-EXP	0.993	0.979	1	0.996	1	1	-	-	-	-
OK-MAT	0.993	0.979	1	0.996	1	1	1	-	-	-
OK-SPH	0.993	0.979	1	0.996	1	1	1	1	-	-
OK-STE	0.993	0.979	1	0.996	1	1	1	1	1	-
TPS	0.993	0.979	1	0.996	1	1	1	1	1	1

Table 7. -- Rank order correlation (Kendall's tau) of cold pool area estimates among methods. OK = ordinary kriging, BES = Bessel, CIR = circular, EXP = exponential, MAT = Matérn, SPH = spherical, STE = Stein's Matérn, IDW = inverse distance weighting, IDW (Max 4) = inverse distance weighting with only four closest observations used for prediction, NN = nearest neighbor, TPS = thin plate spline.

Method	Old	IDW	IDW (Max 4)	NN	OK-BES	OK-CIR	OK-EXP	OK-MAT	OK-SPH	OK-STE
IDW	0.932	-	-	-	-	-	-	-	-	-
IDW (Max 4)	0.963	0.917	-	-	-	-	-	-	-	-
NN	0.960	0.915	0.980	-	-	-	-	-	-	-
OK-BES	0.952	0.929	0.966	0.963	-	-	-	-	-	-
OK-CIR	0.952	0.917	0.977	0.969	0.972	-	-	-	-	-
OK-EXP	0.946	0.923	0.983	0.963	0.972	0.983	-	-	-	-
OK-MAT	0.946	0.923	0.983	0.963	0.972	0.983	1	-	-	-
OK-SPH	0.954	0.926	0.986	0.966	0.969	0.986	0.991	0.991	-	-
OK-STE	0.946	0.923	0.983	0.963	0.972	0.983	1	1	0.991	-
TPS	0.949	0.915	0.98	0.966	0.963	0.98	0.986	0.986	0.977	0.986

Cold Pool Area and Temperature Trends

Trends in survey bottom temperature, surface temperature, and cold pool area are an indicator of ecosystem conditions in the eastern Bering Sea. These trends have been described extensively in the peer-reviewed literature, survey data reports, and annually in EBS Ecosystem Status Reports, Economic and Socioeconomic Profiles for focal stocks, and EBS stock assessments. Because changes to temperature and cold pool area calculations resulted in only minor changes to historical cold pool area and mean temperature estimates, we provide only a brief overview of key patterns and trends here.

From 1982 to 2021, the southeastern Bering Sea underwent substantial variation in annual mean bottom temperatures (mean: 2.50° C, range: 0.70 to 4.37°) and surface temperatures (mean = 6.75°, range: 3.89 to 9.55 °C) during the surveys (Figs. 5 and 6). Before the late 1990s, bottom temperatures fluctuated near the long-term average, where above or below average temperatures were only observed for 1–3 consecutive years. Since the late 1990s, bottom and surface temperatures have had longer "stanzas" of warmer than average and colder than average temperatures. Bottom and surface temperatures were > 0.55 °C above

the time-series average for six out of seven of the most recent years with data (2014 to 2019, 2021) and > 0.76 °C below the long-term average for seven out of eight years from 2006 to 2013. There is strong positive correlation between mean bottom temperature and mean surface temperature (Pearson's $r_{[37]} = 0.83$; $p < 0.001$).

There was considerable variation in the extent of the EBS shelf survey area with bottom temperatures ≤2 °C (i.e., cold pool extent) over the duration of the time series (Figs. 6 and 7). From 1982 to 2021, the mean area of the cold pool was 181,079 km^2 (36.7% of the EBS survey area), with a maximum of 385,975 km^2 (78.2% of survey area) in 1999 and a minimum of 6,150 km^2 (1.2% of survey area) in 2018. Cold pool area trends mirror EBS shelf mean bottom temperature trends, as evidenced by the strong negative correlations between cold pool area and mean bottom temperature ($r_{[37]} = -0.97$; $p < 0.001$). Cold pool area also had a strong negative correlation with mean surface temperature ($r_{[37]} = -0.77$; $p < 0.001$). There were strong correlations between estimated areal extents of 2°C (cold pool), 1°C, 0°C, and -1°C isotherms ($0.84 \leq r_{[37]} \leq 0.96$; all $p < 0.001$).

There was substantial variation in the distribution of the cold pool between the warmest and coldest years (Fig. 8). During cold years (e.g. 1992, 1999, 2012), the cold pool extended over a large proportion of the EBS middle shelf, between 50-m and 100-m isobaths, and into Bristol Bay. During warm years (e.g., 1987, 2003, 2018), the cold pool was limited to the northern edge of the EBS shelf survey area.

The NBS bottom trawl survey was conducted in only four years (2010, 2017, 2019, 2021), three of which were during the warm stanza that began in 2014 in the EBS (Table 2; Figures 5 and 6). The average bottom temperature in 2010 (during the cold stanza) was 1.89 °C. During the warm stanza, average bottom temperatures were 4.38 °C in 2017, 5.63 °C in 2019, and 3.91 °C in 2021. Average surface temperatures were 9.16°C (2010), 9.56° (2017), 10.76 °C (2018), and 8.38 °C (2021). Mean bottom and surface temperatures were not significantly correlated in the NBS ($r_{[2]} = 0.62$; $p = 0.38$), although the time series is likely too short for meaningful statistical inference.

During years when both the EBS shelf and NBS survey were conducted (2010, 2017, 2019, 2021), the area north of 60 °N near Nunivak Island had bottom (Fig. 9) and surface (Fig. 10) temperatures that were several (~3–8 °C) degrees warmer than in the EBS survey region to the immediate south. This transition is not evidence of a dramatic shift in ocean conditions. Rather, the area typically has a fully mixed water column and the temperature difference is a result of solar heating because the NBS stations around Nunivak Island were sampled 34 to 46 days later, on average, than the EBS stations directly to the south (Fig. 1).

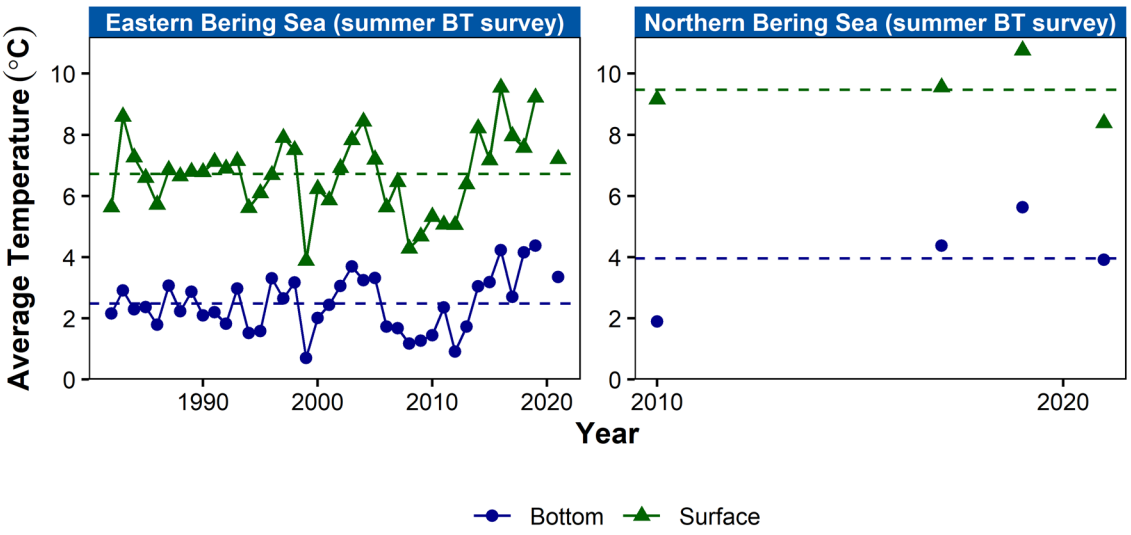

Figure 5. -- Average summer surface (green triangles) and bottom (blue circles) temperature (°C) data products for the eastern Bering Sea (EBS) shelf and northern Bering Sea (NBS). Dashed lines represent the time series mean for the EBS (1982–2021, except 2020) and NBS (2010, 2017, 2019, 2021).

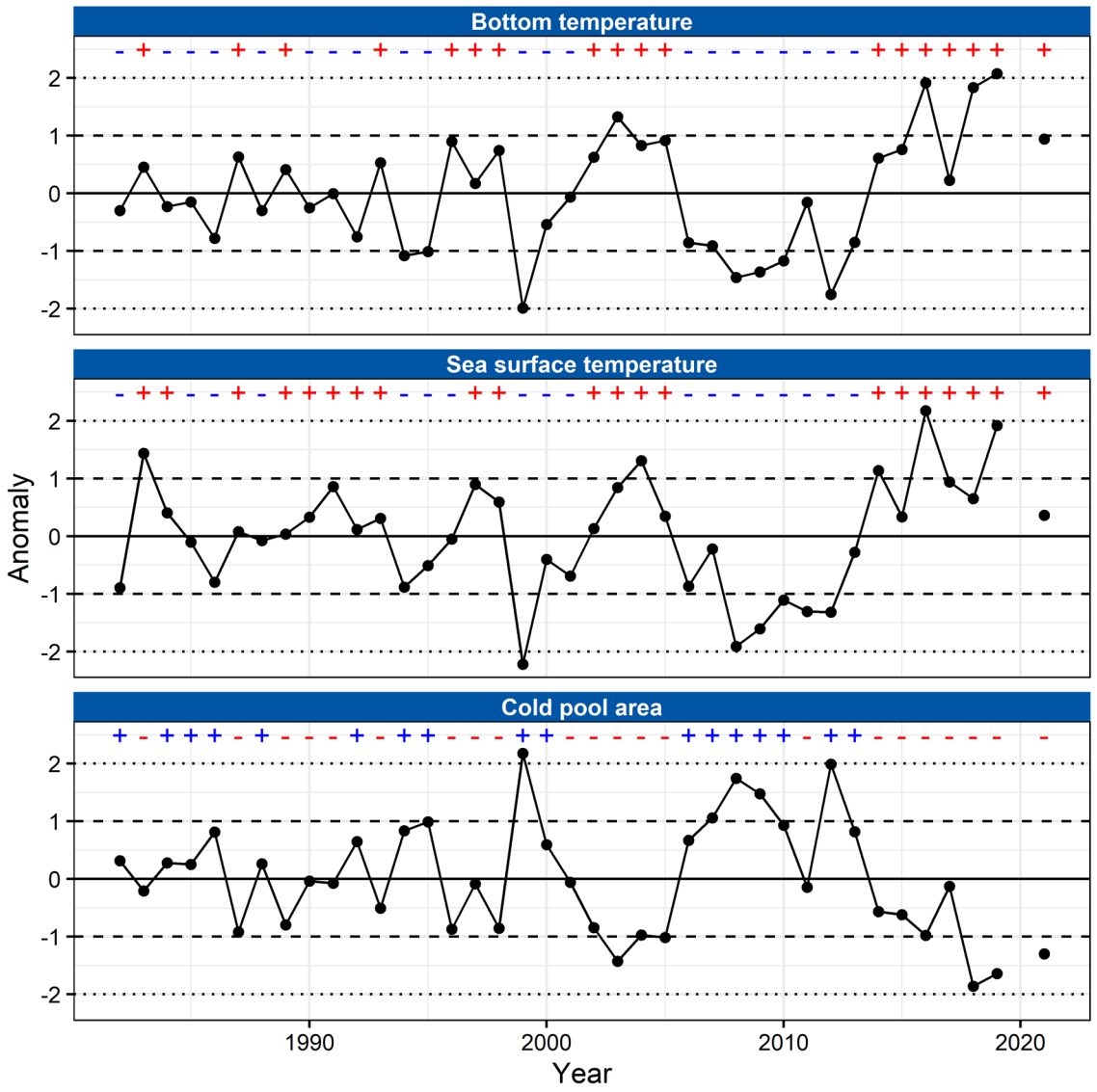

Figure 6. -- Anomalies (Z-score) of mean bottom temperature, sea surface temperature, and cold pool area on the eastern Bering Sea shelf from 1982 to 2021. Lines denote the grand mean (solid line), ±1 standard deviation (dashed lines), ±2 standard deviations (dotted lines). Plus (+) and minus (-) symbols at top denote whether the score is higher or lower than the mean, respectively. Symbol colors denote whether anomalies are associated with warmer (red) or colder (blue) than average conditions.

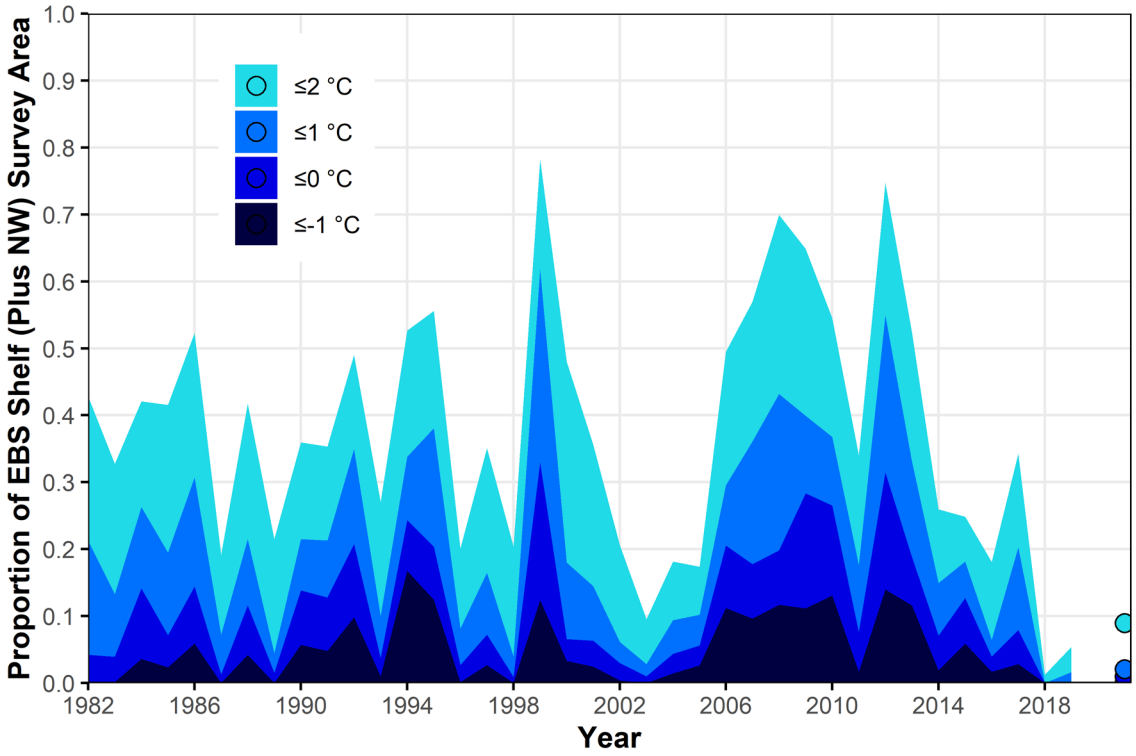

Figure 7. -- Proportion of the southeastern Bering Sea survey area with bottom temperatures ≤ 2°C, ≤ 1°C, ≤ 0°C, and ≤ -1°C.

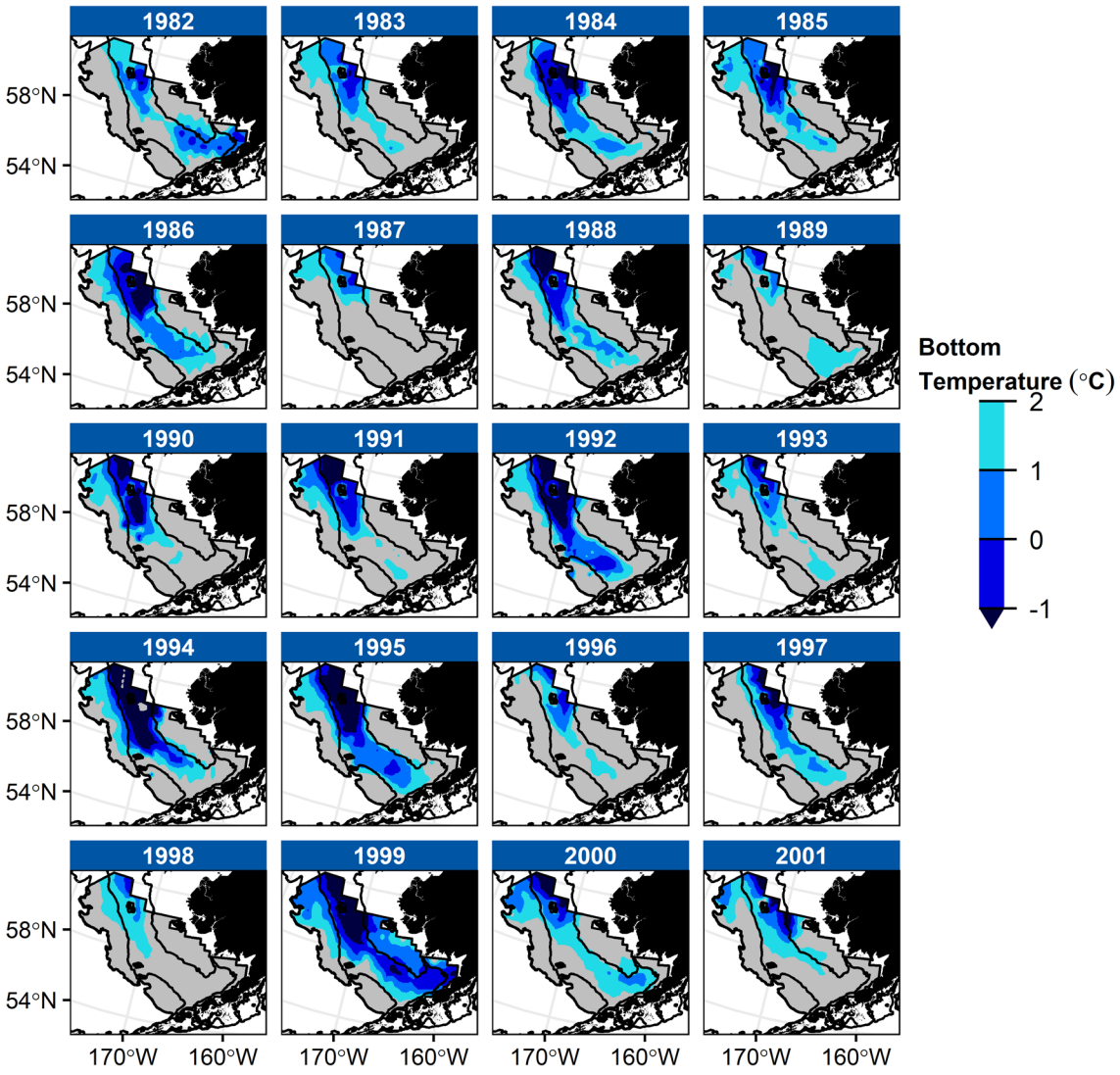

Figure 8. -- Cold pool extent in the eastern Bering Sea from 1982–2021 calculated using ordinary kriging with a Stein's Matérn variogram model (OK-STE). Fill color shows areas with bottom temperatures ≤ 2°C, ≤ 1°C, ≤ 0°C, and ≤ -1°C. Solid black lines show the 50 m, 100 m, and 200 m isobaths.

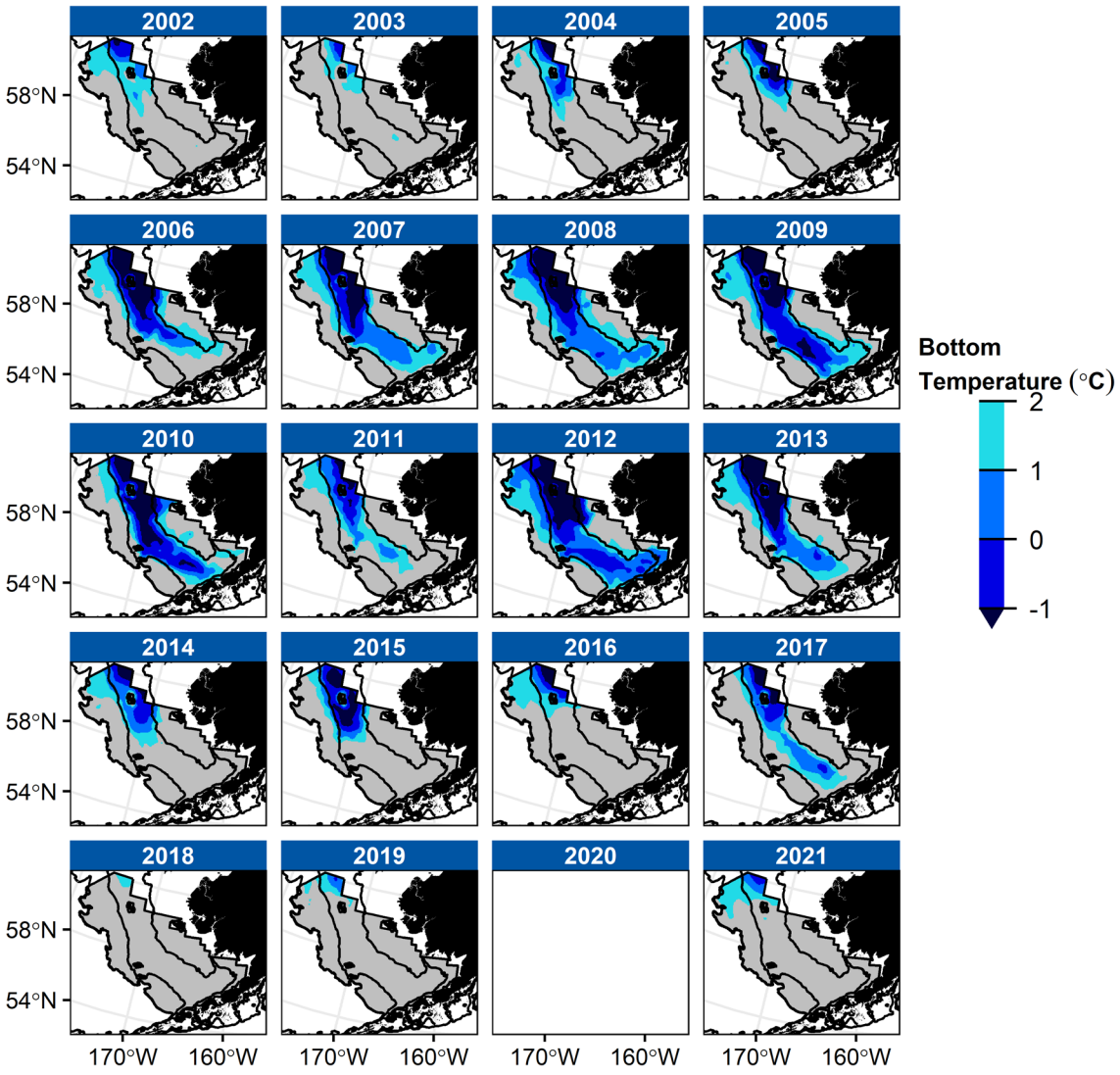

Figure 8. -- Cont.

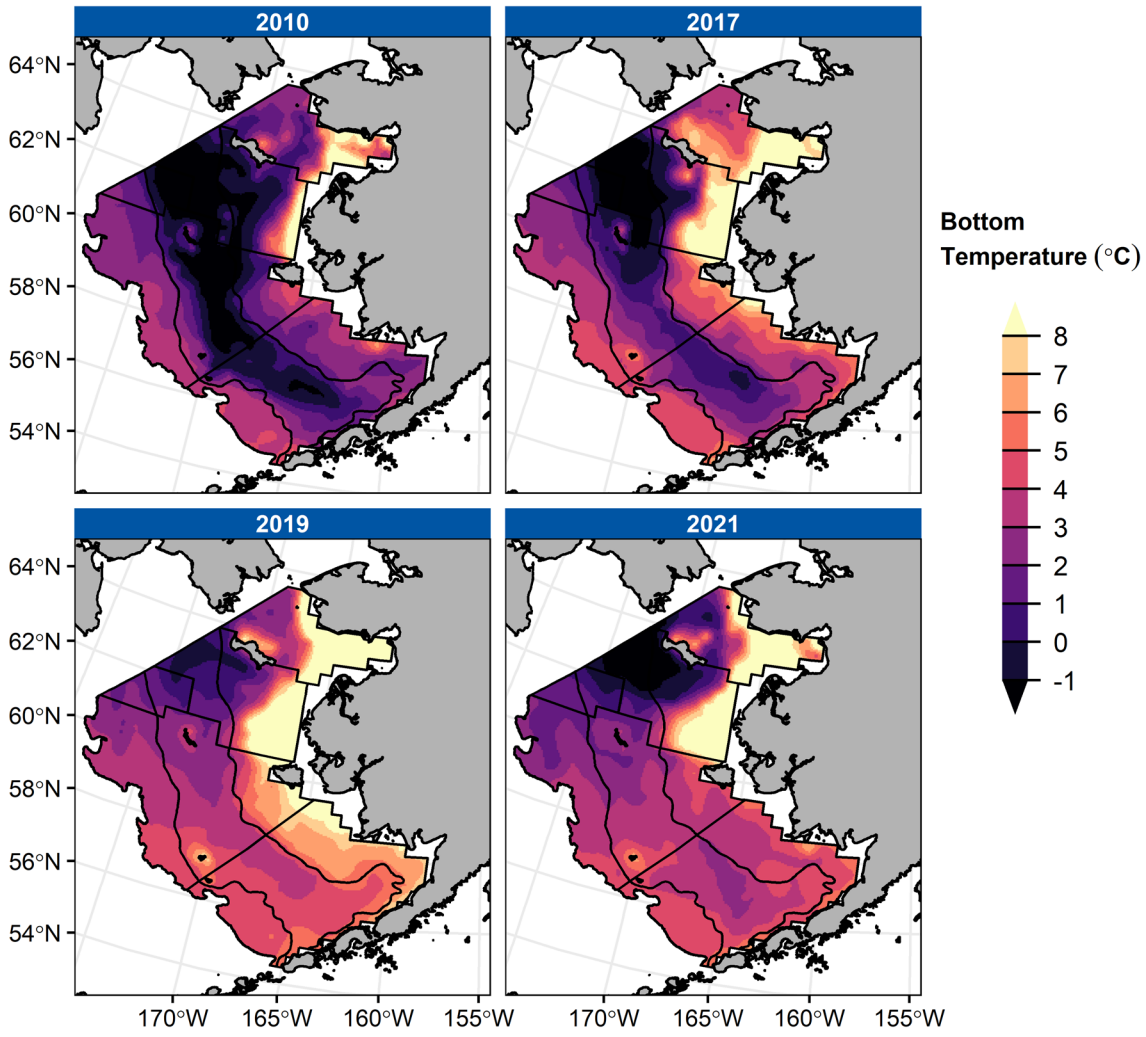

Figure 9. -- Maps of bottom temperature (°C) during years when both the EBS shelf and NBS surveys were conducted (2010, 2017, 2019, and 2021).

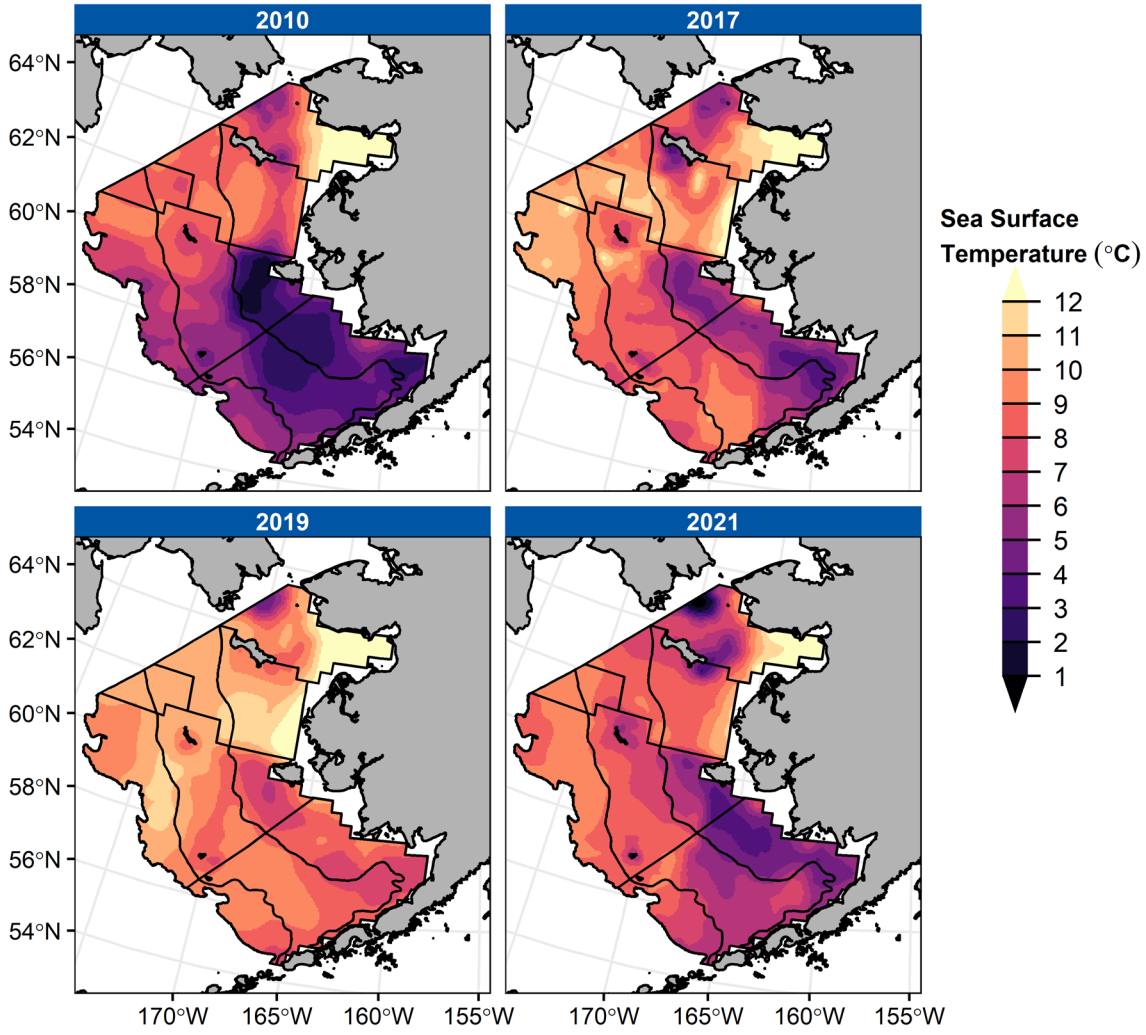

Figure 10. -- Maps of sea surface temperature (°C) during years when both the EBS shelf and NBS surveys were conducted (2010, 2017, 2019, and 2021).

DISCUSSION

Predictive performance varied among interpolation methods; however, estimates of mean bottom temperature and surface temperature were strongly correlated among methods and mostly within 0.05°C of each other. The best performing method for bottom temperature and cold pool area was ordinary kriging with a Stein's Matérn variogram model (OK-STE), while the best performing method for sea surface temperature was inverse distance weighting using

only the four nearest observations (IDW-NMAX4). Although IDW-NMAX4 and thin plate spline slightly outperformed OK-STE, we generated all data products based on interpolation using OK-STE. We opted for this approach to ensure consistency between temperature products and because ordinary kriging is a true geostatistical method that estimates change in autocorrelation with distance. Furthermore, ordinary kriging is presumably less sensitive to outliers that can occur when adjacent stations are sampled at different times or when observation errors occurred due to graphically assisted manual selection of sea surface temperature (Table 1).

Temporal trends in the spatial footprint of the cold pool, along with bottom and surface temperature patterns, indicate the eastern Bering Sea experienced dramatic interannual variability in thermal structure from 1982 to 2021. Recently, the region has experienced two sustained warm phases (2001–2005 and 2014–2021) and one cool phase (2006–2012), with the most recent warm period from 2018 to 2021 associated with historically low seasonal sea-ice extent (Stabeno and Bell 2019). The loss of sea ice is expected to continue in the future due to ongoing effects of climate change. Thus, the EBS region is likely to experience a higher frequency of warm years in the future, similar to that observed from 2018–2021. One major frontier of research, particularly in the subarctic, is understanding how the apparent non-stationarity of both the mean and variance of sea temperatures, attributable to rapid recent warming will affect the abundance, distribution and productivity of stocks (e.g., Ward et al. 2022), let alone indirect effects of species interactions and the environment on ecosystem structure and function (Hollowed et al. in review). For example, these warm conditions, in concert with seasonal sea ice dynamics, affect energy flux through the ecosystem by modifying the phenology and community structure of phytoplankton and zooplankton, which influences horizontal and vertical distribution, condition, survival and recruitment in larval and juvenile fishes (Coyle et al. 2011, Hunt et al. 2011, Duffy-Anderson et al. 2017). Considering the small extent of the cold pool in recent years, it is likely that the bottom temperatures on the eastern Bering Sea shelf have not imposed a major thermal barrier to migration of subarctic species for some time. However, cooler bottom temperatures in the northern Bering Sea may have imposed at least a partial barrier to northward migration in some years.

Temperature and cold pool area data products from EBS shelf summer bottom trawl surveys are currently used as inputs to stock assessment models and to provide contextual information that informs ecosystem-based management of EBS fisheries. Stock assessments for EBS walleye pollock (*Gadus chalcogrammus*) and Pacific cod use cold pool area as a density covariate to account for temperature-dependent variation in bottom-trawl survey catchability (Thompson et al. 2021, Ianelli et al. 2021, Thorson et al. 2020). Similarly, the stock assessment for eastern Bering Sea-Aleutian Islands arrowtooth flounder uses mean bottom temperature as a catchability covariate to account for temperature-driven variation in herding or availability (Shotwell et al. 2020). The stock assessment for EBS yellowfin sole (*Limanda aspera*) uses mean bottom temperature from EBS shelf survey strata with bottom depths < 100 m to correct for variation in catchability that results from temperature-dependent variation in the timing of spawning and feeding migrations (Nichol et al. 2019, Spies et al. 2021). In an appendix to the EBS northern rock sole stock assessment, recruitment is projected using the percentage of northern rock sole nursery habitat within the cold pool because above average bottom temperatures in nursery habitats have been linked to higher recruitment of northern rock sole

Lepidopsetta polyxystra (Cooper et al. 2020, McGilliard et al. 2020). Because temperatures can impose barriers to migration and affect demographic processes (e.g., growth, recruitment, and mortality), trends in temperature and cold pool area data products are discussed in groundfish stock assessment 'risk tables' that qualitatively describe potential stressors on EBS stocks and early warning signs for reduced productivity (Dorn and Zador 2020). Cold pool area and bottom temperature products are also used in suites of quantitative indicators that represent stock vulnerabilities and critical processes in Ecosystem and Socioeconomic Profiles of EBS Pacific cod (Shotwell et al. 2021) and Bristol Bay red king crab (Fedewa et al. 2020a). Finally, cold pool area, bottom temperature, and surface temperature data products are featured prominently in annual Bering Sea Ecosystem Status Reports (Siddon 2021) that provide contextual information about ecosystem conditions to inform stakeholders about ecosystem trends and support ecosystem-based fishery management (Link 2016, Slater et al. 2017).

While bottom trawl survey temperature data products have been used to investigate the effect of temperature on the distribution and migration of groundfish and crab species in the EBS and NBS for decades, recent evidence indicates a need to carefully consider which specific temperature product is most relevant for a given species. Historically, the 2 °C isotherm was hypothesized to be an important temperature threshold for delineating community structure for subarctic and Arctic species (e.g., Wyllie-Echeverria and Wooster 1998). However, recent studies have shown that a more relevant temperature threshold for several subarctic fishes and crabs is the 1 °C isotherm (Kotwicki and Lauth 2013), or the 0°C isotherm for walleye pollock and Pacific cod (Baker 2021, Eisner et al. 2020). While we show a strong correlation between the extent of the 2°C isotherm and other 'cold' isotherms (1°C, 0°C, -1°C), users of EBS shelf and NBS temperature products should consider which temperature product (Appendix) is likely to be biologically or ecologically meaningful for a species or process of interest.

We strongly encourage researchers who use the EBS shelf or NBS temperature products to consider whether the spatial and temporal scale of the data product is appropriate for the intended application. The spatial and temporal scale of observations matters tremendously for detecting, interpreting, and understanding patterns that result from physical and biological processes (Stommel 1964, Levin 1992). The temperature and biological data collected concurrently during EBS shelf and NBS surveys are spatially and temporally aligned observations of in situ temperature, community structure, and demography that is useful for many analyses. However, alternative temperature data products, such as predictions from oceanographic models (e.g., Kearney et al. 2021) or time-adjusted survey temperatures (e.g., Cokelet 2016), may be more appropriate for characterizing conditions depending on the application.

Future research could help identify the extent to which seasonal timing of survey sampling influences temperature data products. Variation in survey start date and the progression of survey sampling over space affects survey temperature measurements because the eastern Bering Sea warms throughout the summer. This warming effect was evident in the temperature differences along the EBS shelf-NBS survey boundary around Nunivak Island. The effect of solar warming on survey data products could be addressed phenomenologically, with statistical models, or mechanistically, by using physical models to account for the solar heating that occurs during the survey. Such confounding effects could potentially be accounted for using a phenomenological approach by implementing universal kriging or related regression approaches to model day of year as a nuisance variable (e.g., as a linear term centered on the

mean sample date across all survey years). Alternatively, a physical model could be used to estimate daily heat flux and vertical mixing within the mixed layer, similar to the method used by Cokelet (2016) to correct temperature data collected using trawl-mounted CTDs during EBS shelf and NBS bottom trawl surveys from 2008–2010. To make the adjustments, Cokelet (2016) estimated an average daily summer (May–August) heat flux of 140 W m^{-2} in the EBS based on Danielson et al.'s (2011) estimate of total summer surface heat flux of 3.0×10^{20} J for an 800 km x 250 km x 45 m parcel on the Bering Sea shelf from 2002 to 2007. Cokelet (2016) estimated the daily temperature increase in the mixed layer ($\Delta T/\Delta d$) was $3.0/z_{ML}$ degrees per day (°C d^{-1}), where z_{ML} is the depth of the surface mixed layer, based on assumptions of no vertical mixing between the surface and deeper layers, surface mixed layer density equal to 1,025 kg m^{-3}, and specific heat equal to 4,020 J kg^{-1} °C^{-1}. Mixed layer depths from TDR vertical temperature profiles could be used as a basis to predict "standardized" date-specific temperatures for the surface mixed layer. These standardized predictions could then be compared with temperature estimates produced using other methods, including ocean models such as the Bering10K ROMS model (Kearney 2021, Kearney et al. 2021).

Combining data products (Appendix) and functions for calculating the data products in an open-source R package promotes reproducibility and scientific transparency (Marwick et al. 2018), consistent with recommendations for improving ecosystem-based fisheries management (Bastille et al. 2021), and ensures users can more easily and reliably access temperature data products from AFSC trawl surveys. Over the past two decades, annual temperature data products from AFSC bottom trawl surveys have been used as indicators of ecosystem variability in the eastern Bering Sea. However, this technical memorandum provides the first detailed description of methods used to generate these data products and this is the first time open-source methods have been used to produce these data products. Furthermore, the new methods are more appropriate for geostatistical analysis and generally provide estimates with improved accuracy relative to historical methods.

ACKNOWLEDGMENTS

We are extremely grateful to Jim Ianelli and Kelly Kearney for providing constructive comments on an earlier version of this manuscript, and Lukas DeFilippo, Stan Kotwicki, and Emily Markowitz for testing and providing feedback on the *coldpool* R package. We thank Lyle Britt, Rebecca Haehn, Bob Lauth, and Dan Nichol for calculating historical temperature data products and providing information about historical calculation methods. We appreciate Heather Kenney and Ned Laman for generously taking time to share their knowledge about historical changes to at-sea data collection software and sampling methods. We express our gratitude to Jim Lee for providing editorial revisions to prepare this manuscript for publication. Finally, this work would not have been possible without the effort of the vessel crews, survey support staff, and scientists who have maintained sampling equipment and collected temperature data since 1982. Reference to trade names does not imply endorsement by the National Marine Fisheries Service, NOAA.

CITATIONS

Baker, M.R. 2021. Contrast of warm and cold phases in the Bering Sea to understand spatial distributions of Arctic and sub-Arctic gadids. Polar Biol. 44:1083–1105. https://doi.org/10.1007/s00300-021-02856-x

Bakkala, R.G. 1981. Population characteristics and ecology of yellowfin sole. In: Hood, D.W. and Calder, J.A., (eds.), The Eastern Bering Sea Shelf: Oceanography and Resources, Volume 1. U.S. Dep. Commer., NOAA Off. Mar. Poll, Assessment, U.S. Gov. Print. Off., Washington, D.C. p. 553-574. https://doi.org/10.5962/bhl.title.61718

Bakkala, R.G., J.J. Traynor., K. Teshima, A.M. Shimada, and H. Yamaguchi. 1985. Results of cooperative U.S.-Japan groundfish investigations in the eastern Bering Sea during June–November 1982. U.S. Dep. Commer., NOAA Tech. Memo. NMFS-F/NWC-87, 448 p.

Bastille, K., S. Hardison, L. deWitt, J. Brown, J. Samhouri, S. Gaichas, S. Lucey, K. Kearney, B. Best, S. Cross, and S. Large. 2020. Improving the IEA approach using principles of open data science. Coastal Manage. 49(1): 72-89. https://doi.org/10.1080/08920753.2021.1846155

Boldt, J. and S. Zador. 2009. Appendix C: Ecosystem Considerations for 2010. *In* Stock Assessment and Fishery Evaluation Report for the Groundfish Resources of the Bering Sea/Aleutian Islands Regions. North Pacific Fishery Management Council, Anchorage, AK. https://apps-afsc.fisheries.noaa.gov/refm/docs/2009/ecosystem.pdf

Buckley, T.W., A., Greig, A., and J.L. Boldt. 2009. Describing summer pelagic habitat over the continental shelf in the eastern Bering Sea, 1982-2006. U.S. Dep. Commer., NOAA Tech. Memo. NMFS-AFSC-196, 49 p.

Cokelet, E.D., 2016. 3-D water properties and geostrophic circulation on the eastern Bering Sea shelf. Deep Sea Res. Part II Top. Stud. Oceanogr. 134: 65–85. https://doi.org/http://dx.doi.org/10.1016/j.dsr2.2016.08.009

Cooper, D., L.A. Rogers, T. Wilderbuer. 2020. Environmentally driven forecasts of northern rock sole (*Lepidopsetta polyxystra*) recruitment in the eastern Bering Sea. Fish. Oceanogr. 29: 111–121. https://doi.org/10.1111/fog.12458

Coyle, K. O., L. Eisner, F. J. Mueter, A. Pinchuk, M. Janout, K. Cieciel, E. Farley, and A. Andrews. 2011. Climate change in the southeastern Bering Sea: impacts on pollock stocks and implications for the Oscillating Control Hypothesis. Fish. Oceanogr. 20:139-156. https://doi.org/10.1111/j.1365-2419.2011.00574.x

Danielson, S.L., O. Ahkinga, C. Ashjian, E. Basyuk, L.W. Cooper, L. Eisner, E. Farley, K.B. Iken, J.M. Grebmeier, L. Juranek, G. Khen, S.R. Jayne, T. Kikuchi, C. Ladd, K. Lu, R.M. McCabe, G.W.K. Moore, S. Nishino, F. Ozenna, R.S. Pickart, I. Polyakov, P.J. Stabeno, R. Thoman, W.J. Williams, K. Wood, T.J., and Weingartner. 2020. Manifestation and consequences of warming and altered heat fluxes over the Bering and Chukchi Sea continental shelves. Deep. Res. Part II Top. Stud. Oceanogr. 177. https://doi.org/10.1016/j.dsr2.2020.104781

Danielson, S., L. Eisner, T. Weingartner, and K. Aagaard. 2011. Thermal and haline variability over the central Bering Sea shelf: Seasonal and interannual perspectives. Cont. Shelf Res. 31: 539–554. https://doi.org/10.1016/j.csr.2010.12.010

Dorn, M.W. and S.G. Zador. 2020. A risk table to address concerns external to stock assessments when developing fisheries harvest recommendations. Ecosyst. Heal. Sustain. 6. https://doi.org/10.1080/20964129.2020.1813634

Duffy-Anderson, J. T., P. J. Stabeno, E. C. Siddon, A. G. Andrews, D. W. Cooper, L. B. Eisner, E. V. Farley, C. E. Harpold, R. A. Heintz, and D. G. Kimmel. 2017. Return of warm conditions in the southeastern Bering Sea: phytoplankton-fish. PloS One 12:e0178955. https://doi.org/10.1371/journal.pone.0178955

Duffy-Anderson, J.T., P. Stabeno, A.G. Andrews III, K. Cieciel, A. Deary, E. Farley, C. Fugate, C. Harpold, R. Heintz, D. Kimmel, K. Kuletz, J. Lamb, M. Paquin, S. Porter, L. Rogers, A. Spear, and E. Yasumiishi. 2019. Responses of the northern Bering Sea and southeastern Bering Sea pelagic ecosystems following record-breaking low winter sea ice. Geophys. Res. Lett. 46: 9833–9842. https://doi.org/10.1029/2019GL083396

Eisner, L.B., Y.I. Zuenko, E.O. Basyuk, L.L. Britt, J.T. Duffy-Anderson, S. Kotwicki, C. Ladd, and W. Cheng. 2020. Environmental impacts on walleye pollock (*Gadus chalcogrammus*) distribution across the Bering Sea shelf. Deep. Res. Part II Top. Stud. Oceanogr. 181–182, 104881. https://doi.org/10.1016/j.dsr2.2020.104881

Fedewa, E., B. Garber-Yonts, and K. Shotwell. 2020. Appendix E: Ecosystem and Socioeconomic Profile of the Bristol Bay Red King Crab Stock. *In* Stock Assessment and Fishery Evaluation Report for BSAI Crab Stocks. 2020 Crab SAFE. North Pacific Fishery Management Council, Anchorage, AK. https://meetings.npfmc.org/CommentReview/DownloadFile?p=ea0403bc-6544-4241-bf8c-b9c7a8ebf17d.pdf&fileName=App_E_BBRKC_ESP_2020.pdf

Fedewa, E.J., T.M. Jackson, J.I. Richar, J.L. Gardner, and M.A. Litzow. 2020. Recent shifts in northern Bering Sea snow crab (*Chionoecetes opilio*) size structure and the potential role of climate-mediated range contraction. Deep Sea Res. Part II Top. Stud. Oceanogr. 181–182, 104878. https://doi.org/10.1016/j.dsr2.2020.104878

Francis, R.C. and K.M. Bailey. 1983. Factors affecting recruitment of selected gadoids in the northeast Pacific and east Bering Sea, p. 35-60. *In* Wooster, W.S. (ed.), From year to year: Interannual variability of the environment and fisheries of the Gulf of Alaska and the eastern Bering Sea. Washington Sea Grant, University of Washington, Seattle, WA. https://repository.library.noaa.gov/view/noaa/37252

Grüss, A., J.T. Thorson, C.C. Stawitz, J.C.P. Reum, S.K. Rohan, and C.L. Barnes. 2021. Synthesis of interannual variability in spatial demographic processes supports the strong influence of cold-pool extent on eastern Bering Sea walleye pollock (*Gadus chalcogrammus*). Prog. Oceanogr. 194, 102569. https://doi.org/10.1016/j.pocean.2021.102569

Hollowed, A., L. Barnett, T. Gelatt, A. Haynie, K. Shotwell, E. Siddon, R. Angliss, E. Fedewa, K. Holsman, J. Duffy-Anderson, S. Parker-Stetter, T. Honkalehto, S. Kotwicki, R. Sewall, P. Stabeno, and E. Ward. Eastern Bering Sea Regional Action Plan to Implement the NOAA Fisheries Climate Science Strategy in 2022–2024. In review. U.S. Dep. Commer., NOAA Tech. Memo.

Hunt, Jr., G.L., K. O. Coyle, L. B. Eisner, E.V. Farley, R.A. Heintz, F. Mueter, J.M. Napp, J.E. Overland, P.H. Ressler, S. Salo, and P.J. Stabeno. 2011. Climate impacts on eastern Bering Sea foodwebs: a synthesis of new data and an assessment of the Oscillating Control Hypothesis. ICES J. Mar. Sci. 68: 1230-1243. https://doi.org/10.1093/icesjms/fsr036

Ianelli, J.N., T. Buckley, T. Honkalehto, G. Walters, and N. Williamson. 2001. Eastern Bering Sea walleye pollock stock assessment. *In* Stock assessment and fishery evaluation report for the groundfish resources of the Bering Sea/Aleutian Islands Regions. North Pacific Fishery Management Council, Anchorage, Alaska. https://apps-afsc.fisheries.noaa.gov/refm/docs/2001/BSpollock.pdf

Ianelli, J., B. Fissel, S. Stienessen, T. Honkalehto, E. Siddon, C. Allen-Akselrud. 2021. Chapter 1: Assessment of the walleye pollock stock in the eastern Bering Sea. *In* Stock assessment and fishery evaluation report for the groundfish resources of the Bering Sea/Aleutian Islands Regions. North Pacific Fishery Management Council, Anchorage, Alaska. https://apps-afsc.fisheries.noaa.gov/refm/docs/2021/EBSPollock.pdf

Kearney, K. 2021. Temperature data from the eastern Bering Sea continental shelf bottom trawl survey as used for hydrodynamic model validation and comparison. U.S. Dep. Commer., NOAA Tech. Memo. NMFS-AFSC-415, 40 p. https://doi.org/10.25923/e77k-gg40

Kearney, K.A., M. Alexander, K. Aydin, W. Cheng, A.J. Hermann, G. Hervieux, and I. Ortiz. 2021. Seasonal predictability of sea ice and bottom temperature across the eastern Bering Sea shelf. J. Geophys. Res. Ocean. 126, 1–21. https://doi.org/10.1029/2021JC017545

Kotwicki, S. and R. R. Lauth. 2013. Detecting temporal trends and environmentally-driven changes in the spatial distribution of bottom fishes and crabs on the eastern Bering Sea shelf. Deep Sea Res. Part II: Top. Stud. Oceanogr. 94: 231-243. https://doi.org/10.1016/j.dsr2.2013.03.017

Ladd, C. and P.J. Stabeno. 2012. Stratification on the eastern Bering Sea shelf revisited. Deep Sea Res. Part II Top. Stud. Oceanogr. 65–70: 72–83. https://doi.org/10.1016/j.dsr2.2012.02.009

Lauth, R. and E. Acuna. 2007. 2005 bottom trawl survey of the eastern Bering Sea continental shelf. AFSC Processed Rep. 2007-1, 164 p. Alaska Fish. Sci. Cent., NOAA, Natl. Mar., Fish. Serv., 7600 Sand Point Way NE, Seattle, WA 98115. https://repository.library.noaa.gov/view/noaa/8596

Lauth, R.R. and E. Acuna. 2007. Results of the 2006 eastern Bering Sea continental shelf bottom trawl survey of groundfish and invertebrate resources. U.S. Dep. Commer., NOAA Tech. Memo. NMFS-AFSC-176, 175 p. https://repository.library.noaa.gov/view/noaa/22890

Lauth, R.R., E.J. Dawson, J. Conner. 2019. Results of the 2017 eastern and northern Bering Sea continental shelf bottom trawl survey of groundfish and invertebrate fauna. U.S. Dep. Commer., NOAA Tech. Memo. NMFS-AFSC-396, 260 p. https://doi.org/10.25923/h118-nw41

Levin, S.A. 1992. The problem of pattern and scale in ecology. Ecology 73: 1943–1967. https://doi.org/doi:10.2307/1941447

Link, J. S. 2016. NOAA Fisheries ecosystem-based fisheries management road map. National Oceanic and Atmospheric Administration, National Marine Fisheries Service, NMFSI-01-120-01, Washington, D.C. https://media.fisheries.noaa.gov/dam-migration/01-120-01.pdf

Livingston, P. (Ed.). 1999. Appendix D: Ecosystem Considerations for 2000. *In* Stock Assessment and Fishery Evaluation Report for the Groundfish Resources of the Bering Sea/Aleutian Islands Regions. North Pacific Fishery Management Council, Anchorage, AK. https://apps-afsc.fisheries.noaa.gov/refm/docs/historic_assess/ecocons99.pdf

Marwick, B., C. Boettiger, and L. Mullen. 2018. Packaging data analytical work reproducibly using R (and friends). Am. Stat. 72:80–88. https://doi.org/10.1080/00031305.2017.1375986

McGilliard, C.R., J. Ianelli, A.E. Punt, T. Wilderbuer, D. Nichol, and R. Haehn. 2020. Assessment of the northern rock sole stock in the Bering Sea and Aleutian Islands. *In* Stock Assessment and Fishery Evaluation Report for the Groundfish Resources of the Bering Sea/Aleutian Islands Regions. North Pacific Fishery Management Council, Anchorage, AK. https://apps-afsc.fisheries.noaa.gov/refm/docs/2020/BSAIrocksole.pdf

Mueter, F.J., C. Ladd, M.C. Palmer, and B.L. Norcross. 2006. Bottom-up and top-down controls of walleye pollock (*Theragra chalcogramma*) on the Eastern Bering Sea shelf. Prog. Oceanogr. 68:152–183. https://doi.org/10.1016/j.pocean.2006.02.012.

Mueter, F.J., and M.A. Litzow. 2008. Sea ice retreat alters the biogeography of the Bering Sea continental shelf. Ecol. Appl. 18:309–320. https://doi.org/10.1890/07-0564.1

Nichol, D.G., S. Kotwicki, T.K. Wilderbuer, R.R. Lauth, and J.N. Ianelli. 2019. Availability of yellowfin sole *Limanda aspera* to the eastern Bering Sea trawl survey and its effect on estimates of survey biomass. Fish. Res. 211: 319–330. https://doi.org/10.1016/j.fishres.2018.11.017

Pebesma, E.J. 2004. Multivariable geostatistics in S: the gstat package. Computers & Geosciences 30:683-691. https://doi.org/10.1016/j.cageo.2004.03.012

Rogers, L., D. Cooper, and T. Wilderbuer. 2020. Appendix E. Estimating Northern Rock Sole recruitment using environmental covariates. *In* Stock assessment and fishery evaluation report for the groundfish resources of the Bering Sea/Aleutian Islands Regions. North Pacific Fishery Management Council, Anchorage, Alaska. https://apps-afsc.fisheries.noaa.gov/refm/docs/2020/BSAIrocksole.pdf

Shotwell, S.K., I. Spies, L. Britt, M. Bryan, D.H. Hanselman, D.G. Nichol, J. Hoff, W. Palsson, T.K. Wilderbuer, and S. Zador. 2020. Assessment of the arrowtooth flounder stock in the eastern Bering Sea and Aleutian Islands. *In* Stock assessment and fishery evaluation report for the groundfish resources of the Bering Sea/Aleutian Islands Regions. North Pacific Fishery Management Council, Anchorage, Alaska. https://apps-afsc.fisheries.noaa.gov/refm/docs/2020/BSAIatf.pdf

Shotwell, S.K., G.G. Thompson, B. Fissel, T. Hurst, B. Laurel, L. Rogers, E. Siddon, and A. Tyrell. 2021. Appendix 2.2: Ecosystem and Socioeconomic Profile. *In* Stock assessment and fishery evaluation report for the groundfish resources of the Bering Sea/Aleutian Islands Regions. North Pacific Fishery Management Council, Anchorage, Alaska. https://apps-afsc.fisheries.noaa.gov/refm/docs/2021/EBSpcod.pdf

Siddon, E. (ed.). 2021. Ecosystem status report 2021: eastern Bering Sea. *In* Stock assessment and fishery evaluation report for the groundfish resources of the Bering Sea/Aleutian Islands Regions. North Pacific Fishery Management Council, Anchorage, Alaska. https://apps-afsc.fisheries.noaa.gov/refm/docs/2021/EBSecosys.pdf

Siddon, E.C., T. Kristiansen, F.J. Mueter, K.K.Holsman, R.A. Heintz, and E.V. Farley. 2013. Spatial match-mismatch between juvenile fish and prey provides a mechanism for recruitment variability across contrasting climate conditions in the eastern Bering Sea. PLoS One 8:13. https://doi.org/10.1371/journal.pone.0084526

Slater, W., G. DePiper, J. Gove, C. Harvey, E. Hazen, S. Lucey, M. Karnauskas, S. Regan, E. Siddon, E. Yasumiishi, et al. 2017. Challenges, opportunities and future directions to advance NOAA Fisheries ecosystem status reports (ESRs): Report of the National ESR Workshop. U.S. Department of Commerce, NOAA Tech. Memo. NMFS-F/SPO-174. https://repository.library.noaa.gov/view/noaa/17422/noaa_17422_DS1.pdf

Spencer, P.D. 2008. Density-independent and density-dependent factors affecting temporal changes in spatial distributions of eastern Bering Sea flatfish. Fish. Oceanogr. 17:396–410. https://doi.org/10.1111/j.1365-2419.2008.00486.x.

Spencer, P.D., K.K. Holsman, S. Zador, N.A. Bond, F.J. Mueter, A.B. Hollowed, and J.N. Ianelli. 2016. Modelling spatially dependent predation mortality of eastern Bering Sea walleye pollock, and its implications for stock dynamics under future climate scenarios. ICES J. Mar. Sci. 73: 1330–1342. https://doi.org/10.1093/icesjms/fsw040

Stabeno, P.J., and S.W. Bell. 2019. Extreme conditions in the Bering Sea (2017–2018): record-breaking low sea-ice extent. Geophys. Res. Lett. 46:8952–8959. https://doi.org/10.1029/2019GL083816

Stabeno, P.J., E.V. Farley, N.B. Kachel, S. Moore, C.W. Mordy, J.M. Napp, J.E. Overland, A.I. Pinchuk, and M.F. Sigler. 2012. A comparison of the physics of the northern and southern shelves of the eastern Bering Sea and some implications for the ecosystem. Deep. Res. Part II Top. Stud. Oceanogr. 65–70: 14–30. https://doi.org/10.1016/j.dsr2.2012.02.019

Stauffer, G. 2004. NOAA protocols for groundfish bottom trawl surveys of the nation's fishery resources. U.S. Dep. Commerce, NOAA Tech. Memo. NMFS-F/SPO-65, 205 p. https://spo.nmfs.noaa.gov/sites/default/files/tm65.pdf

Stommel, H. 1963. Varieties of oceanographic experience. Science. 139 (3555): 572–576. https://doi.org/10.1126/science.139.3555.572

Thompson, G.G., S. Barbeaux, J. Conner, B. Fissel, T. Hurst, B. Laurel, C.A. O'Leary, L. Rogers, S.K. Shotwell, E. Siddon, I. Spies, J.T. Thorson, and A. Tyrell. Assessment of the Pacific cod stock in the eastern Bering Sea. *In* Stock assessment and fishery evaluation report for the groundfish resources of the Bering Sea/Aleutian Islands Regions. North Pacific Fishery Management Council, Anchorage, Alaska. https://apps-afsc.fisheries.noaa.gov/refm/docs/2021/EBSpcod.pdf

Thorson, J.T., L. Ciannelli, and M.A. Litzow. 2020. Defining indices of ecosystem variability using biological samples of fish communities: A generalization of empirical orthogonal functions. Prog. Oceanogr. 181. https://doi.org/10.1016/j.pocean.2019.102244.

United States Department of Commerce. 1983. Cruise results: NOAA R/V *Chapman* Cruise CH-83-03, R/V *Alaska* AK 83-01. Northwest and Alaska Fish. Cent., NOAA, Natl. Mar., Fish. Serv., 2725 Montlake Blvd. E., Seattle, WA 98112. https://origin-archive-afsc.fisheries.noaa.gov/RACE/surveys/cruise_archives/cruises1983/results_AK-CH1983-01_03.pdf

United States Department of Commerce. 1984. Cruise results: NOAA R/V *Chapman* Cruise CH-84-04, R/V *Alaska* AK 84-01, eastern Bering Sea crab groundfish survey. Northwest and Alaska Fish. Cent., NOAA, Natl. Mar., Fish. Serv., 7600 Sand Point Way NE, Bin C15700, Bldg. 4, Seattle, WA https://apps-afsc.fisheries.noaa.gov/RACE/surveys/cruise_archives/cruises1984/results_AK-CH1984-01_04.pdf

United States Department of Commerce. 1992. Cruise results: Cruise 92-1 Alaska, Cruise 92-1 Tracy Anne, Cruise 92-1 *Mys Babushkina*, 1992 eastern Bering Sea crab and groundfish survey, June–August 1992. Alaska Fish. Sci. Cent., NOAA, Natl. Mar., Fish. Serv., 7600 Sand Point Way NE, Bin C15700, Bldg. 4, Seattle, WA 98115.https://apps-afsc.fisheries.noaa.gov/RACE/surveys/cruise_archives/cruises1992/results_1992_AL01_TA01_MBB01.pdf

von Szalay, P.G., and D.A. Somerton. 2005. The effect of net spread on the capture efficiency of a demersal survey trawl used in the eastern Bering Sea. Fish. Res. 74:86–95. https://doi.org/10.1016/j.fishres.2005.04.007

Walters, G (compiler). 1996. 1992 bottom trawl survey of the eastern Bering Sea continental shelf. AFSC Processed Report 96-05, 164 p. Alaska Fish. Sci. Cent., NOAA, Natl. Mar., Fish. Serv., 7600 Sand Point Way NE, Seattle, WA 98115.https://apps-afsc.fisheries.noaa.gov/Publications/ProcRpt/PR1996-05.pdf

Ward, E.J., L.A.K. Barnett, S.C. Anderson, C.J.C. Commander, and T.E. Essington. 2022. Incorporating non-stationary spatial variability into dynamic species distribution models. ICES J. Mar. Sci. 79: 2422–2429.

Wilderbuer, T.K. and D. Nichol. 2001. Yellowfin sole. *In* Stock assessment and fishery evaluation report for the groundfish resources of the Bering Sea/Aleutian Islands Regions. North Pacific Fishery Management Council, Anchorage, Alaska. https://apps-afsc.fisheries.noaa.gov/refm/docs/2001/BSyfs.pdf

Wyllie-Echeverria, T. and W.S. Wooster. 1998. Year-to-year variations in Bering Sea ice cover and some consequences for fish distributions. Fish. Oceanogr. 7: 159–170. https://doi.org/10.1046/j.1365-2419.1998.00058.x

APPENDIX: DATA PRODUCTS

Appendix Table A1. -- Eastern Bering Sea continental shelf and northern Bering Sea mean bottom temperature (BT), mean sea surface temperature (SST), and isotherm area (e.g., cold pool area) data products in the *coldpool* R package.

Product Name	Data Set in Package	Extent	Data Used
EBS shelf area with BT ≤ 2°C (i.e., cold pool area), km^2	cold_pool_index$AREA_LTE2_KM2	EBS Shelf incl. NW strata	Gear temperature from EBS shelf standard index stations (including corner stations), 1982–present
EBS shelf area with BT ≤ 1°C, km^2	cold_pool_index$AREA_LTE1_KM2	EBS Shelf incl. NW strata	Gear temperature from EBS shelf standard index stations (including corner stations), 1982–present
EBS shelf area with BT ≤ 0°C, km^2	cold_pool_index$AREA_LTE0_KM2	EBS Shelf incl. NW strata	Gear temperature from EBS shelf standard index stations (including corner stations), 1982–present
EBS shelf area with BT ≤ -1°C, km^2	cold_pool_index$AREA_LTEMINUS1_KM2	EBS Shelf incl. NW strata	Gear temperature from EBS shelf standard index stations (including corner stations), 1982–present
EBS shelf mean BT, °C	cold_pool_index$MEAN_BOTTOM_TEMPERATURE	EBS Shelf incl. NW strata	Gear temperature from EBS shelf standard index stations (including corner stations), 1982–present
EBS shelf mean SST, °C	cold_pool_index$MEAN_SURFACE_TEMPERATURE	EBS Shelf incl. NW strata	Surface temperature from EBS shelf standard index stations (including corner stations), 1982–present
EBS shelf mean BT for strata with bottom depth <100 m, °C	cold_pool_index$MEAN_BT_LT100M	EBS Shelf strata (10, 20, 31, 32, 41, 42, and 43	Gear temperatures from EBS standard index station samples (including corner stations), 1982–present
NBS mean BT, °C	nbs_mean_temperature$MEAN_BOTTOM_TEMPERATURE	NBS	Gear temperature from EBS shelf and NBS standard index stations (including corner stations), 2010–present
NBS mean SST, °C	nbs_mean_temperature$MEAN_SURFACE_TEMPERATURE	NBS	Surface temperature from EBS shelf, and NBS standard index stations (including corner stations), 2010–present

Appendix Table A2. -- Bottom temperature (BT) and sea surface temperature (SST) raster grids in the *coldpool* R package.

Product Name	Data Set in Package	Extent	Data Used
EBS shelf BT raster 5 x 5 km grid, °C	ebs_bottom_temperature	EBS Shelf incl. NW strata	Gear temperature from EBS shelf standard index stations (including corner stations), 1982–present
EBS shelf SST raster 5 x 5 km grid, °C	ebs_surface_temperature	EBS Shelf incl. NW strata)	Gear temperature from EBS shelf standard index stations (including corner stations), 1982–present
EBS shelf + NBS BT raster 5 x 5 km grid, °C	nbs_ebs_bottom_temperature	EBS Shelf incl. NW strata + NBS	Gear temperature from EBS shelf and NBS standard index stations (including corner stations), 2010–present
EBS shelf + NBS SST raster 5 x 5 km grid, °C	nbs_ebs_surface_temperature	EBS Shelf incl. NW strata + NBS	Surface temperature from EBS shelf, and NBS standard index stations (including corner stations), 2010–present

Appendix Table A3. -- Deprecated historical mean bottom temperature (BT), mean sea surface temperature (SST), and isotherm area (e.g., cold pool area) data products in the *coldpool* R package.

Product Name	Data Set in Package	Extent	Data Used
EBS shelf area with BT ≤ -1°C, km^2	cpa_pre2021$AREA_KM2_MINUS_1	EBS shelf without NW strata	Gear temperature from EBS shelf standard stratum index stations (excluding corner stations), 1982–2019
EBS shelf area with -1°C < BT ≤ 0°C, km^2	cpa_pre2021$AREA_KM2_0	EBS shelf without NW strata	Gear temperature from EBS shelf standard stratum index stations (excluding corner stations), 1982–2019
EBS shelf area with 0°C < BT ≤ 1°C, km^2	cpa_pre2021$AREA_KM2_1	EBS shelf without NW strata	Gear temperature from EBS shelf standard stratum index stations (excluding corner stations), 1982–2019
EBS shelf area with 1°C < BT ≤ 2°C, km^2	cpa_pre2021$AREA_KM2_2	EBS shelf without NW strata	Gear temperature from EBS shelf standard stratum index stations (excluding corner stations), 1982–2019
EBS shelf area with BT ≤ 0°C, km^2	cpa_pre2021$AREA_SUM_KM2_LTE0	EBS shelf without NW strata	Gear temperature from EBS shelf standard stratum index stations (excluding corner stations), 1982–2019
EBS shelf area with bottom temperature ≤ 1°C, km^2	cpa_pre2021$AREA_SUM_KM2_LTE1	EBS shelf without NW strata	Gear temperature from EBS shelf standard stratum index stations (excluding corner stations), 1982–2019
EBS shelf area with bottom temperature ≤ 2°C (i.e., cold pool extent), km^2	cpa_pre2021$AREA_SUM_KM2_LTE2	EBS shelf without NW strata	Gear temperature from EBS shelf standard stratum index stations (excluding corner stations), 1982–2019
EBS standard area-weighted mean BT, °C	cpa_pre2021$AVGBST_STANDARD	EBS shelf without NW strata	Gear temperature from EBS shelf standard stratum index stations (excluding corner stations), 1982–2021
EBS standard area-weighted mean SST, °C	cpa_pre2021$AVGSST_STANDARD	EBS shelf without NW strata	Surface temperature from EBS shelf standard stratum index stations (excluding corner stations), 1982–2021

Product Name	Data Set in Package	Extent	Data Used
EBS standard + NW area-weighted mean BT, °C	cpa_pre2021$AVGBSBT_PLUSNW	EBS shelf incl. NW strata	Gear temperature from EBS shelf standard stratum index stations (excluding corner stations), 1982–2021
EBS standard + NW area-weighted mean SST, °C	cpa_pre2021$AVGBSST_PLUSNW	EBS shelf incl. NW strata	Surface temperature from EBS shelf standard stratum index stations (excluding corner stations), 1982–2021
NBS area-weighted mean BT, °C	cpa_pre2021$AVGBSBT_NBS	NBS	Gear temperature from NBS index stations, 2010–2021
NBS area-weighted mean SST, °C	cpa_pre2021$AVGBSST_NBS	NBS	Surface temperature from NBS index stations, 2010–2021
EBS mean BT for stations < 100 m bottom depth, °C	cpa_pre2021$AVGBSBT_LT100M	EBS Shelf incl. NW strata	Bottom temperature from EBS shelf standard stratum samples from depths < 100 m, 1982–2021
EBS mean SST for stations < 100 m bottom depth, °C	cpa_pre2021$AVGBSST_LT100M	EBS Shelf incl. NW strata	Surface temperature from EBS shelf standard stratum samples from depths < 100 m, 1982–2021

U.S. Secretary of Commerce
Gina M. Raimondo

Under Secretary of Commerce for Oceans and Atmosphere
Dr. Richard W. Spinrad

Assistant Administrator, National Marine Fisheries Service. Also serving as Acting Assistant Secretary of Commerce for Oceans and Atmosphere, and Deputy NOAA Administrator
Janet Coit

December 2022

www.nmfs.noaa.gov

OFFICIAL BUSINESS

National Marine Fisheries Service
Alaska Fisheries Science Center
7600 Sand Point Way N.E.
Seattle, WA 98115-6349